Technical Support for the Long-Term Deployment of an L-Band Radiometer at Concordia Station

Yearly Report – Data Acquisition and Processing Report
Third Year – D3- D6
June 2016

EUROPEAN SPACE AGENCY STUDY
ESTEC Contract 4000105872/12/NL/NF

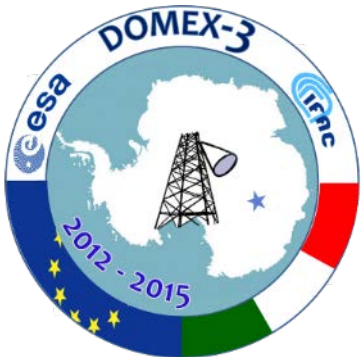

Prepared by

Giovanni MACELLONI, Marco BROGIONI, Simone Pettinato, Francesco Montomoli
IFAC- CNR, Florence, ITALY

DATE: 13/10/2016
Version: 2.0
Deliverable of the contract: D6-D3

Consiglio Nazionale delle Ricerche
Istituto di **F**isica **A**pplicata "Nello **C**arrara"
VIA MADONNA DEL PIANO N. 10 - CAP 50019 SESTO FIORENTINO FIRENZE

This page is intentionally left blank

ESA STUDY CONTRACT REPORT

ESTEC CONTRACT NO:	SUBJECT:		CONTRACTOR:
4000105872/12/NL/NF	Technical Support for the Long-Term Deployment of an L-Band Radiometer at Concordia Station		IFAC
ESA CR ( )NO:	STAR CODE:	No of volumes: 1 This is volume no: 1	CONTRACTOR'S REF: Deliverable

ABSTRACT:

PREPARED BY:

GIOVANNI MACELLONI, MARCO BROGIONI, SIMONE PETTINATO, FRANCESCO MONTOMOLI -IFAC

ESA STUDY MANAGER:	ESA BUDGET HEADING:
TANIA CASAL	

DOCUMENT CHANGE LOG

Issue/ Revision	Date	Observations
1/0	June 2016	First issue –Draft Version
2/0	October 2016	Second version: the version has been modified after the comments provided by ESA in August 2016

ABBREVIATIONS

AEP	Annual Executive Project
AWS	Automatic Weather Station
CVA-ARABBA	Avalanche Center of Arabba, Italy
ESA	European Space Agency
IASH	International Association of Scientific Hydrology
IFAC-CNR	Institute of Applied Physics – National Research Council
INGV	Istituto Nazionale di Geofisica e Vulcanologia
IOP	Intensive Operational Period
MZS	Mario Zucchelli Station
NOP	Normal Operational Period
OMT	OrthoMode Transducer
PNRA	Programma Nazionale RIcerche in Antartide
RFI	Radio Frequency Interference
RR	Readiness Review Document – D1 of the contract
TEC	Total Electron Content

This page is intentionally left blank.

TABLE OF CONTENTS

1 Purpose and structure of document

Purpose

This document contains the Third Year Report for DOMEX-3 experiment, prepared by the Institute for Applied Physics "Nello Carrara" – Firenze within the framework of the ESA contract N. 4000105872/12/NL/NF.

In the document is described the execution of the activity carried out in the third experimental year of the project (i.e. from January 2015 to December 2015). It includes the description of the third summer campaign 2015-2016 as well as the activity conducted during third year of the winter campaign and in Italy.

The document is divided into sections in which the individual points were discussed.

2 Overview

The Domex-3 experiment is the follow on of two previous experiments called Domex-1 and Domex-2 which were successfully conducted at Concordia base, Antarctica, by IFAC-CNR in cooperation to ESA (contracts N. 18060/04/NL/CB [1] and N. 22046/08/NL/EL, 20066/06/NL/EL [2]) and PNRA.

The results obtained in these contracts demonstrated that DOME- C represents a unique “high”-temperature (i.e. higher than 150 K), extended target that provides a temporally-stable reference which potentially meets existing requirements for assessing the long-term stability of space-borne L-band radiometric instruments.

In order to meet this objective, co-located ground measurements are required in order to verify target stability over time and to monitor changes in target characteristics that may affect the long-term reference signal: for example, surface roughness or “crusting”, which in spite of being quite stable, appears to evolve with time (possibly due to climatic changes) and may affect the brightness temperature. Long-term monitoring of DOME-C is also crucial to investigating further and to modeling variations in H-pol observed during the DOMEX-2 experiment. A long-term experiment is also recommended in order to provide a continuous data record of ground-based radiometric measurements covering the SMOS – Aquarius – SMAP era. The resulting data set will support the Level 1C quality assessment for SMOS and SMAP at the accuracy level required for climate applications. In addition, the produced data set will be instrumental for satellite sensor product intercalibration ensuring an harmonized Level 1 data set of passive microwave observations at L-band for future climate applications.

The objective of DOMEX-3 project is to contribute to the long-term deployment of an L-Band Radiometer at Concordia Station. The activity of the contract is divided in four phases: the first phase deals with the preparation of the instrument and the experiment while the others 3 phases are constituted by the campaign and the analysis of the data acquired during the 3 campaigns 2013, 2014 and 2015. Phase-1 of the activity was devoted to the preparation of an improved version of the L-band microwave radiometer RADOMEX as well as the definition of acquisition procedure and campaign execution. Phase-1 started in January 2012 and ended in October 2012, the performed activities were reported in the CIP and RR document of the contract [3],[4],[5].

Phase-2 of the activity is constituted by the deployment of the instrument during the first summer Antarctic campaign 2012, the acquisition of the data during 2013 and its analysis and the preparation for the Austral summer campaign 2013. It started in November 2012 and ended in October 2013. Results are presented in the First Year Report of the project [6].

Phase-3 of the activity is the subject of this document, it includes the execution of the Antarctic summer campaign from 2013 to 2016. In particular, this document deals to the description of summer campaign 2015-2016 and the data acquisition and analysis for year 2015.

The different sections of the document describe the execution of the summer campaign 2015 and the activities conducted in Antarctica and in Italy during the austral winter. The data acquisition and analysis (D3) is also contained here, the collection of the photographic material is contained in the D4 of the project and the data are contained in D5.

3 The 2015-16 Summer Antarctic Campaign

The third Antarctic campaign of the Domex-3 project was funded by the Italian programme for research in Antarctica - PNRA in the framework of the Monitoring Antarctic Ice Sheet using Advanced Remote Sensing Systems - MAISARS project (PNRA project 2013/AC3.07) leaded by IFAC-CNR. The objective of the project is to investigate on the structure and the properties of the ice sheet at Concordia Station by means of different remote sensing sensors and to inter-compare the obtained results. DOMEX-3 experiment is part of the project.

The 2015 Antarctic campaign of MAISARS involved the maintenance of RADOMEX and the installation of new remote sensing instruments. In the same campaign snow measurements were carried out by using conventional and innovative techniques.

3.1 Description of the campaign

The 2015-16 summer campaign of the PNRA MAISARS project started on November, 9nd 2015. On this date Marco Brogioni from IFAC-CNR and Fabiano Monti Univeristy of Insubria left Italy to reach Christchurch (New Zealand). On Nov, 13th they reached Mario Zucchelli Station (MZS) on the LC130 airplane. The last part of the journey from MZS to Concordia Station (CS) took place on Nov, 15th. This date can be considered the starting date of the summer campaign of the project (the third for Domex-3). On November 21st Vitale Stanzione - CNR arrived at Dome C and joined the project team. The planned tasks of the campaign are:

- maintenance of the L-band microwave radiometer RADOMEX (ESA Domex 3 project),
- deployment of the GNSS reflectometer and interferometer instrument on the tower (ESA GRAIS project –PNRA MAISARS project),
- realignment of the snow temperature probes buried in the snowpack for the monitoring of snow temperature, and maintenance of the datalogger,
- digging of several snow pit for the execution of conventional measurements and collection of IR pictures of the pits walls,
- support to the execution of the radio echo sounding measurements,
- deployment of the Ultra Wide-Band software-defined RADiometer - UWBRAD radiometer (NASA IIT UWBRAD project),
- training of Vitale Stanzione who is the winterover scientist in charge of the Domex 3 and GRAIS projects.

The entire month of November was characterized by a cold and windy weather which makes very difficult to operate outdoor and especially on the observation tower. Moreover some activities were carried out in a heated laboratory (“spare” time tent) . In detail the GRAIS antenna and the UWBRAD instrument were assembled and configured to operate on the station LAN. After the initial harnessing, both GRAIS and UWBRAD were tested outside the tent in order to verify their proper functioning in the Antarctic environment. After that GRAIS had passed all the tests, on Nov 22nd it was moved to the American tower and deployed on the top on Nov 30th. The antenna was oriented towards North-East to observe the area chosen for the intercalibration of GRAIS data, the ground radio echo sounding and conventional measurements. Then, on Dec. 30th the antenna was rotated in the definitive direction (north-west) towards

the clean area over which GRAIS will perform the winter acquisitions in parallel to Radomex. Figure 1 shows pictures of GRAIS antennas deployment.

The maintenance of RADOMEX went quite smooth and consisted essentially in the substitution of the internal RF receiver and the antenna cables and the installation of an extension cable for the PT100 probes which measure the temperature of antenna's cables. The operation was planned to be executed directly on the tower in order to avoid a long period of loss of data. Due to the bad weather condition it was possible to operate the substitution only on Nov, 26th when the wind speed decreased. The RF section was replaced as planned and, at the same time, the installation of an extension cable for the PT100 probes was performed. The installation of this cable was motivated by the previous difficult in substituting the PT100 in case of failure during the winter time. Unfortunately probes didn't work immediately and it was reconnected on Dec,13th. After this last operation the systems of RADOMEX resulted all nominal. The antenna cables were successfully substituted on Jan, 26th by Vitale Stanzione who was accurately trained for this operation. The delay in the substitution was due to the delay in the shipment of the cable by the company (Times Microwave Co). It's worth mentioning that the antenna cables were substituted in order to reduce the dependency of phase and losses modifications to temperature variation.

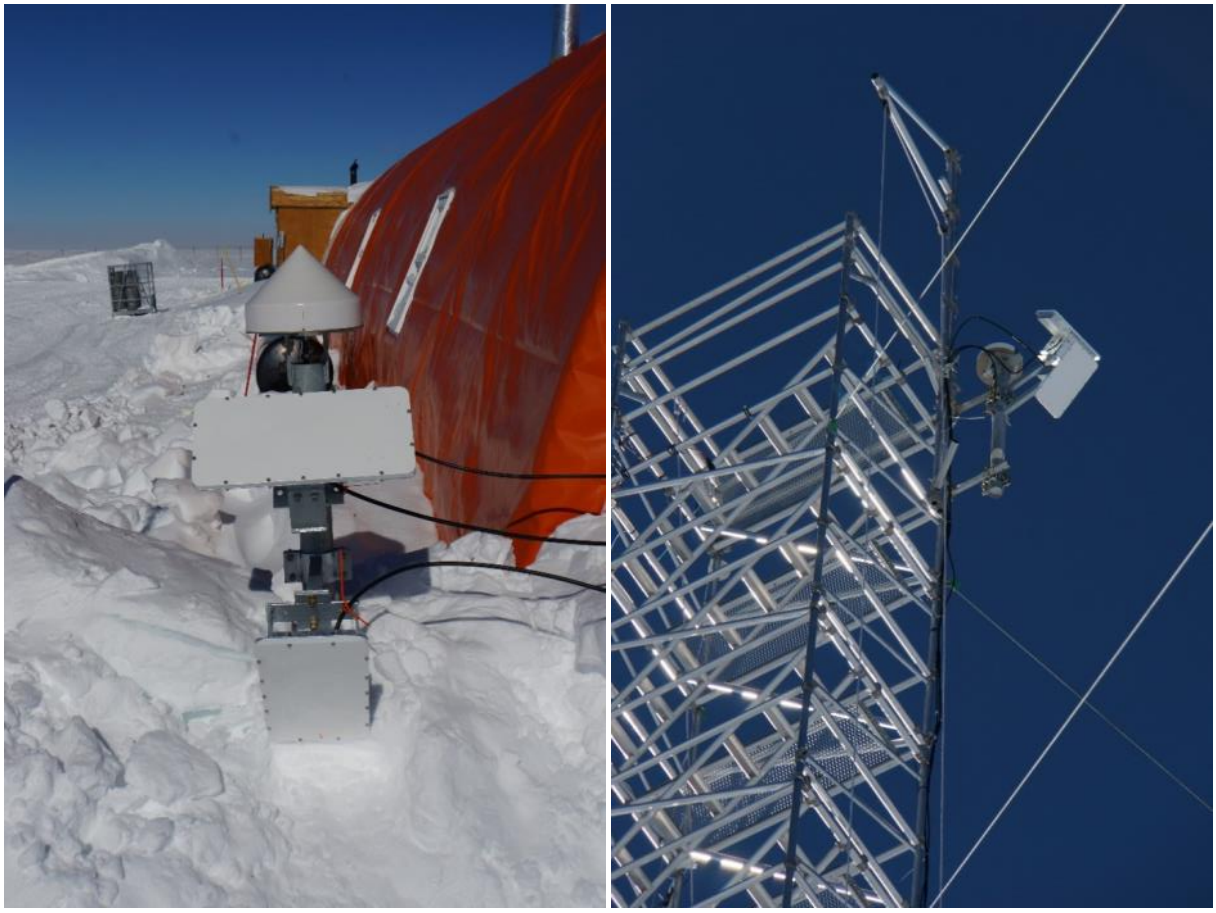

Figure 1 Deployment of GRAIS antenna and preliminary tests (Left), mounting of the antenna in the observation tower (right)

Figure 2 Internal view of the BOX containing the RADOMEX instrument.

Figure 2 represents an internal view of the box containing RADOMEX. Box in grey/red in figure is the RF section. The small box in the red circle is the new i/o PT100 interface whit the extension cable. It was, at the end, placed in a different position with respect to the figure.

UWBRAD radiometer was kept on the ground until mid-December to observe the sky for calibration purposes because of some technical issues in the instrument (Figure 3). After some essential e.m. compatibility measurements performed by the Concordia ICT staff at the beginning of December, the issues were solved and the instrument was ready to be installed on the tower. On Dec. 21st UWBRAD radiometer was installed on the tower: the receiver box was put on the balcony towards the base and the antenna installed at 20m height (just above Radomex). UWBRAD acquired data continuously until the end of the month, when it was moved to the ground for another sky calibration and then switched off on Dec, 31st .

An overview of the observation tower with all the instruments deployed is shown in Figure 4.

Figure 3 UWBRAD instrument observing clear sky.

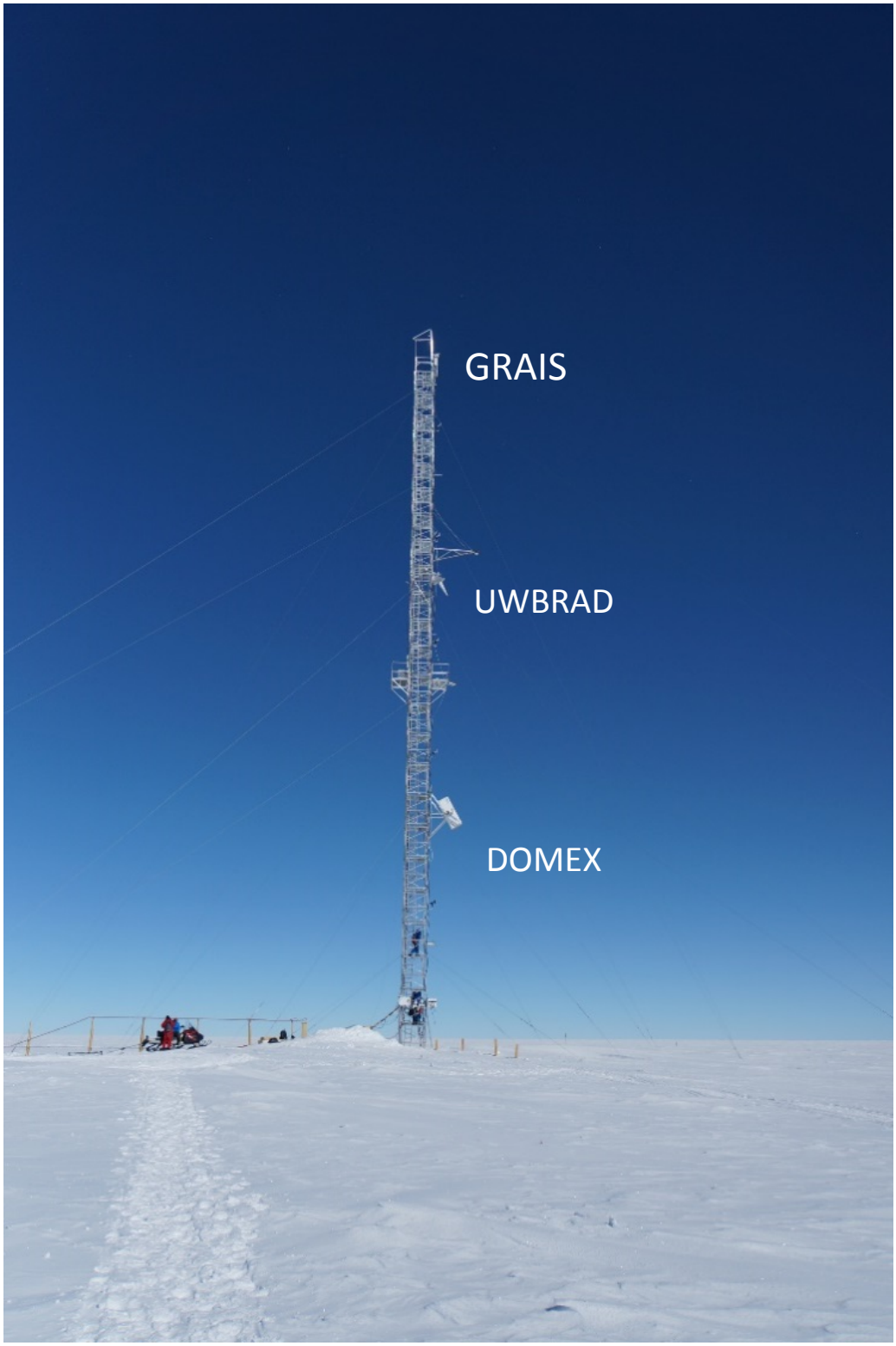

Figure 4 The Concordia's observation tower with DOMEX, UWBRAD and GRAIS.

The realignment of the snow temperature probes was performed on two different days. On Dec, 4th the snow probes were unburied and put all at the same depth of 1 meter for calibration purposes (Figure 5). The snow accumulation occurred since the last campaign measured. The snow accumulation resulted to be

22.5 cm over 2 years. On Dec, 9th the calibration was finished and the maintenance of the datalogger performed. First of all, the temperature probes that were damaged (albeit still working) were substituted with new ones. Then, the insulation of the datalogger box was improved by adding new layers of Styrofoam to the existing internal insulation. After these operations the PT100 probes were put in the snow at the nominal depth and the probes buried again.

During the month of December, when the weather conditions improved, the team started the ground measurements. The activity consisted in digging several snow pits with an average dimension of 3mx3mx2.5m and then collecting high resolution NIR images of the walls orthogonal and parallel to the prevalence-wind direction. Indeed, the NIR data acquired can be used to derive maps of the specific surface area – SSA of the snow crystals and to analyze their spatial variability. Then, after the NIR imaging, conventional measurements were carried out (i.e. profiles of grain size, density and stratigraphy). The pits were dug in the clean area far from the tower in north and south directions to avoid the perturbation of the site observed by the remote sensing instruments. An example of picture's collection is provided in Figure 6.

Figure 5 The PT100 probes placed at the same depth for calibration purposes.

Figure 6 Example of collection of NIR picture in a snow pit

Besides these main activities, the project team was in charge of the set-up of the procedure for transmission of data to Italy, the analysis of the data collected by the instruments and on ground. It is worth noting that for data transfer it was used the so called “Hermes” system which is the new file transfer system installed at Concordia Station since 2014. It allows the transfer of high volumes of data (several hundreds of MB) by using the rsync and SSH protocols. The data transfer takes place at night when the upload bandwidth is almost free. The protocol has been implemented both for GRAIS and for DOMEX. For the GRAIS project it has been granted the transfer of approx. 100 MB per day, while for DOMEX we are still using the old way of data shipment (by e-mail) and we are keeping Hermes as a backup.

The campaign ended on Jan,3th when Marco Brogioni and Fabiano Monti left Concordia Station onboard of the Twin Otter and arrived in Italy on Jan,17th and 16th respectively.

3.2 Activity with the winterover researchers

In order to allowing the proper continuation of Domex-3 and GRAIS, Vitale Stanzione was accurately trained to operate the instruments, to access their internal computer, to download and ship the data. Also, Vitale is in charge of the routinely snow surveys, thus Fabiano Monti taught and trained him the techniques for performing the snow conventional measurements correctly. In particular, the measurements he carried out along the winter season are:

- daily precipitation particles and fresh snow (daily);
- snow accumulation (weekly);

- superficial snow density: 8 samples at 10 cm below the surface in the surroundings of the snow poles for the seasonal accumulation estimation (bi-weekly)
- first meter snow density at 10 cm steps (monthly).

4 DOMEX-3 - 2015 DATA ANALYSIS

4.1 Data acquisitions

RADOMEX acquisitions from January 1 2015 to December 31 2015 are presented in this section. The radiometer continuously acquired during the entire period excepting a small interruption (5 days) from 26 November to 1st December when the receiver was substituted. In the period 1st January - 1st December, the internal calibration of the radiometer was reconfigured with the noise source as a reference after the cold load damage occurred in August 2014. This configuration is described in details in report [6] and in [7]. As explained in the previous section the new receiver was installed in the 2015 summer campaign. This latter use the 2013-2014 calibration scheme which is based on the acquisition of two reference loads placed at two different temperatures as described in detail in [5] , [6].

4.2 Data calibration

The data processing procedure applied to data as acquired by the RADOMEX system can be summarized in three different steps:

1. Reconstruction of corrupted data
2. Tb correction for cable thermal variation (see deliverable [7] for the detailed procedure)
3. Absolute calibration (sky observation and intercalibration with previous data)

4.2.1 Reconstruction of corrupted data

The Tb raw data (i.e. not calibrated) acquired in 2015 are depicted in Figure 7. The Tb time series is very regular until 17th April at both V and H polarizations , and in line with 2013 and 2014 data behaviour. From the end of April until the end of the receiver operations (November 25th) unexpected Tb jumps are observed at V- polarization. The H- pol is more regular until September 9th when some occasional anomalies occurred. A similar behavior can be observed if the antenna counts are represented (Figure 8). These latter represent (in arbitrary unit) the power received by the system from the antenna before the calibration procedure. If we consider the measurements, always expressed in arbitrary counts, collected on the reference loads in the same period (Figure 9) it can be observed that in the period April 17 – September 9 the signal is more regular and doesn't show similar anomalies. It's worth mentioning here that the receiver is composed by a single RF chain allowing to the amplification and detection of the signal coming from antenna ports and reference loads. From above considerations it can be concluded that the anomalies are not due to a receiver's problem or calibration issues but to a malfunctioning of the SP4T

switch connecting the antenna and the calibration outputs. In particular it can be concluded that the problem is related to SP4T port connecting the V polarization, to the receiver RF chain.

Moreover a problem in the antenna cable was also excluded because on November 26, when the receiver was substituted but not the cables, the problem disappeared. In addition, from September 9 similar spikes are also observed in the calibration data (Figure 9) confirming a degradation of the switch's performances.

After the receiver substitution, the normal functioning is restored at both V and H polarizations.

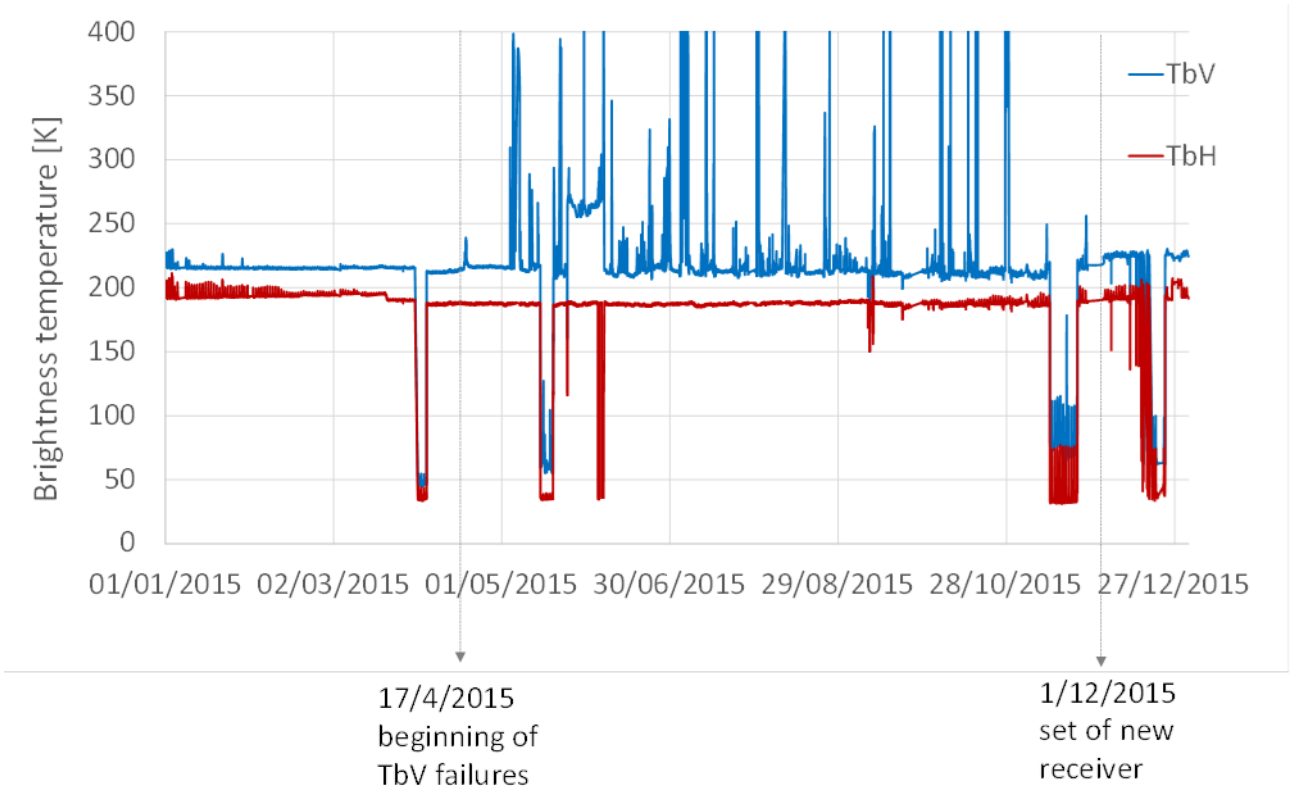

Figure 7: Raw data of brightness temperature recorded on 2015 for V-pol (in blue) and H-pol (in red).

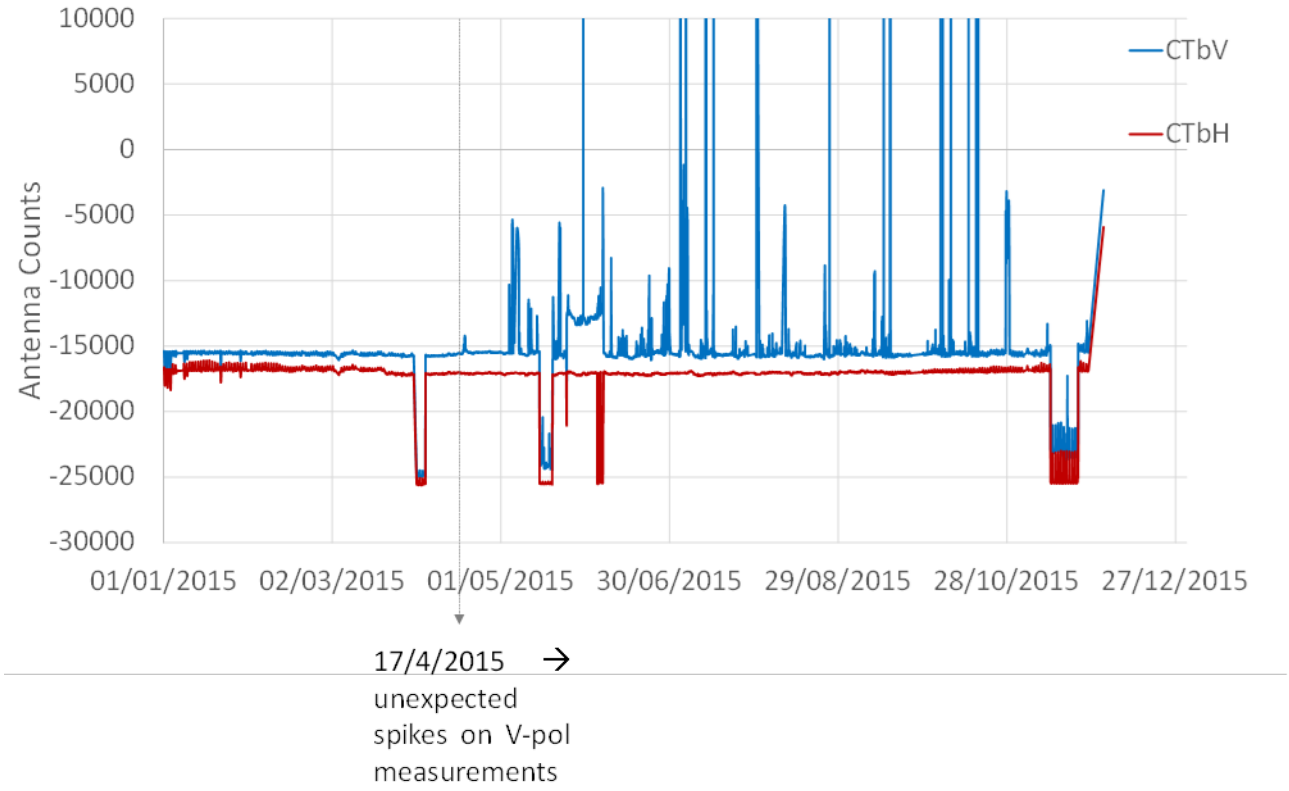

Figure 8: Antenna counts measured at the end of the receiving chain.

Starting from these considerations a strategy to recover the data of the V-pol channel and correct the unexpected jumps observed in the calibration channel after September 9th has been developed

First of all the entire 2015 time series can be divided into four periods:

- In the first period (1/1/2015-17/4/2015) the Tb data have been calculated with the standard procedure, using the frequent calibration technique with the hot load and the noise source as reference, explained in [5]and [6]. The acquired data are averaged over 20 samples during the whole period.

- In the second period (18/4/2015-9/9/2015) the TbV anomalies are very frequent and showing peak values higher than 250K. Because of the random characteristics of the switch failures and the numerous spikes present in each of the 20 sample window, we develop a criterion to select the data. A first selection of TbV is performed using a threshold of 0.5 K on the standard deviation computed over the 20 samples. Among the 20 samples the data that doesn't satisfy the condition were excluded and the average was re-computed on the remaining ones. The procedure is applied only if the number of samples is higher than 7 otherwise the data are filtered out from the series. Moreover, in order to remove the erroneous trends in the series, we used a sliding window filter with a peak-to-peak threshold of 2K.

  For this period, data at H polarization have been processed as in the first period.

Figure 10 shows an example of how V –pol data are corrected. In figure original data are represented with a green line while corrected ones in blue. Figure shows that sporadic spikes are removed and data are excluded from the temporal series when the number of failures is too high.

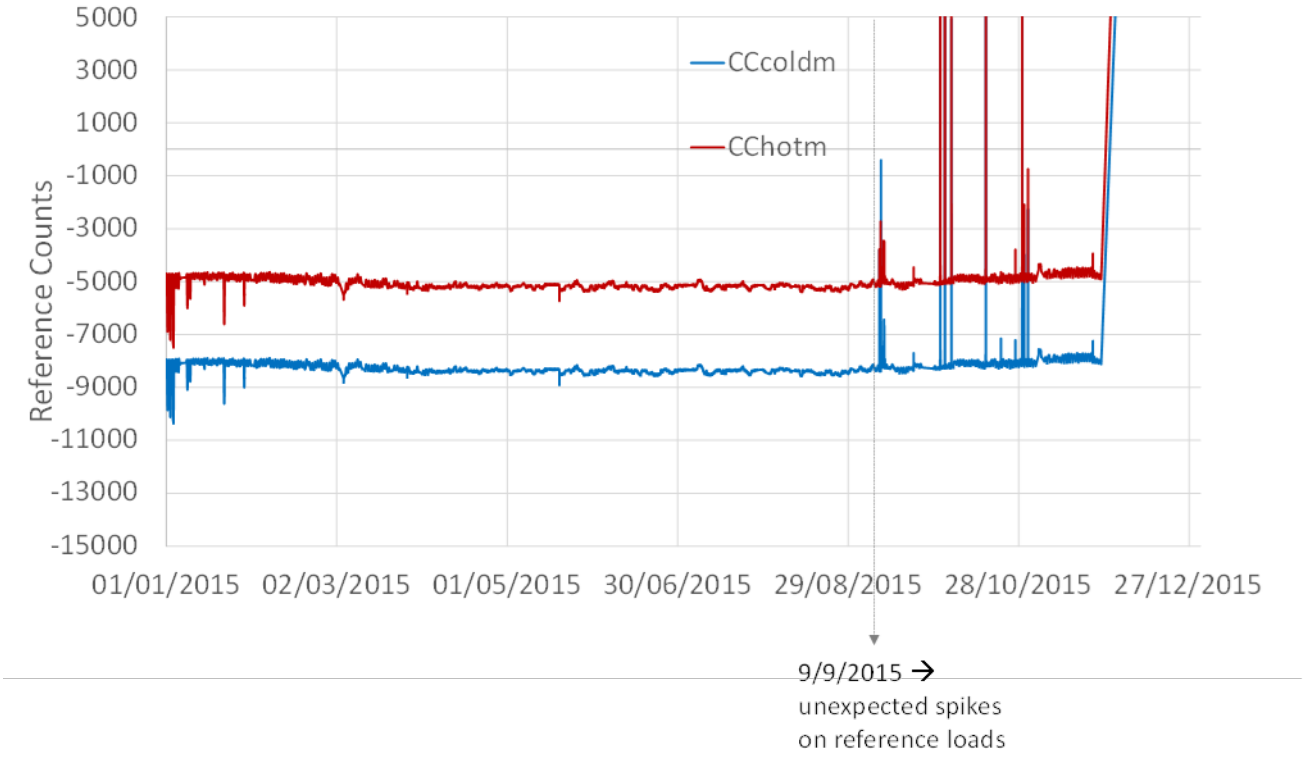

Figure 9: Reference counts used for the internal calibration. The calibration mode is with the noise source as a reference load.

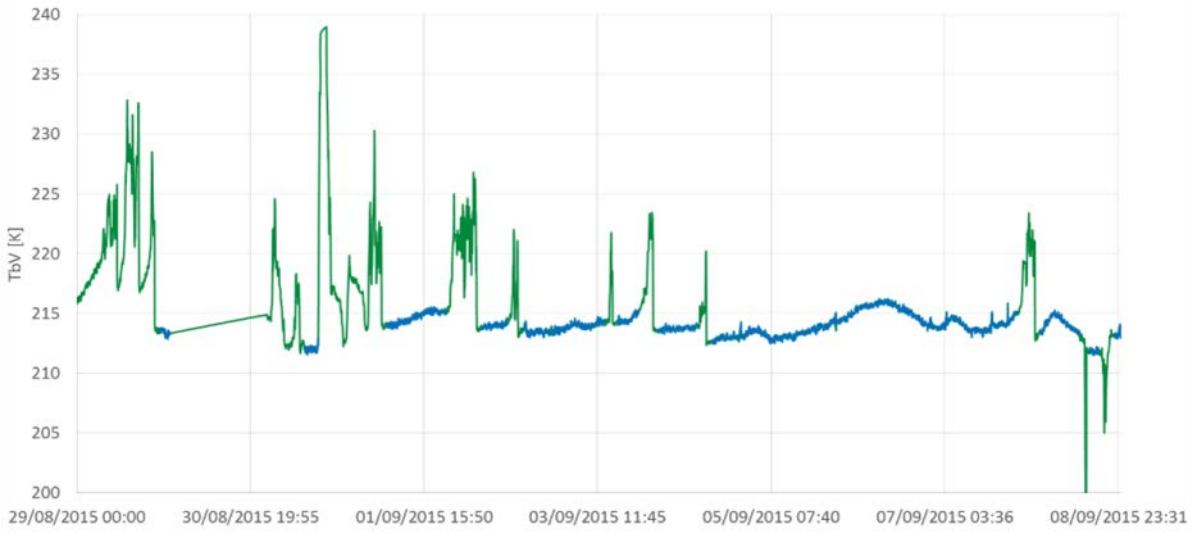

Figure 10: Tb at V- pol in the original data (green) and the data after filtering and averaging (blue)

- In the period (9/9/2015-25/11/2015) a small number of anomalies are also observed at both H and V polarization. As previously explained this is motivated by a problem occurred in the calibration measurements over the reference loads (Figure 9). In order to clean the calibration from random spikes it was established that when spikes are observed a fixed value of gain and offset, were assumed to be equal to the last computed ones, was used. Because offset and gain are computed every 4 minutes and we have verified that the gain and offset remains stable within this time period we expect that data quality are not affected by this assumption. If spikes are observed in consecutive measurements data were excluded. Figure 11 shows an example of the reconstructed value of gain and offset. Once gain and offset are computed V and H-pol data are processed separately, by means of the procedure used for the previous periods.
- From 1/12/2015 – to 31/12/2015 (i.e. after the receiver substitution) the standard processing is adopted at both V- and H- pol.
-

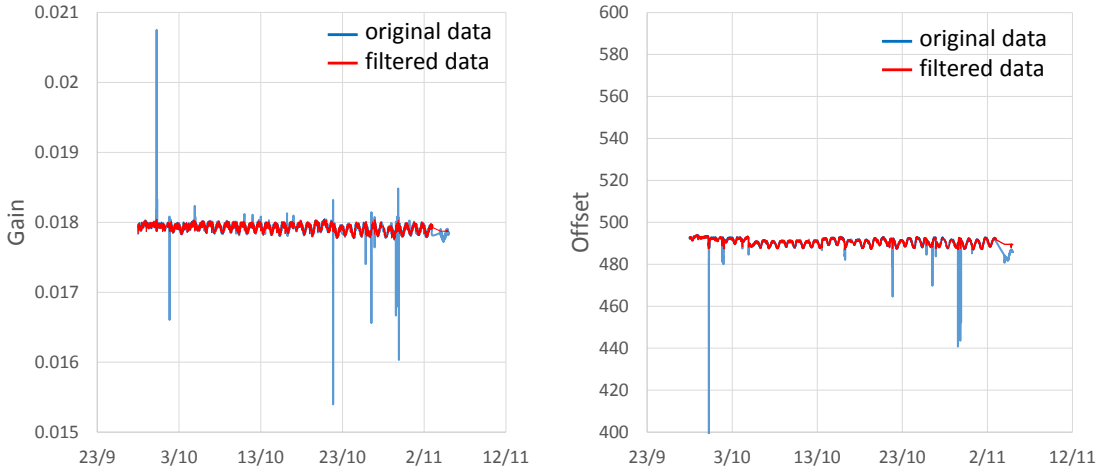

Figure 11: Gain and Offset used for the internal calibration calculated from reference measurements, in blue the original data and in red the filtered ones.

4.2.2 Tb correction from the cable thermal variation

The second step of the data processing is the compensation of thermal variations of cables and connectors located out of the thermo-regulated part of the receiver. The procedure described in details in [6] is not repeated here. Temperatures are measured by the PT100 probes placed on the antenna cables (T1 and T2 for V and H pol respectively) and on the RF cables in the receiver enclosure. On 19/5 the T2 stopped functioning, and, because the correction procedure requires T2 measures, we infer its value from T3. For this purpose it has been used a linear relationship between T2 and T3 which has been computed in a similar thermal conditions. The T2 probe was replaced during the 2015/16 summer campaign.

An example of Tb before and after the thermal correction is shown in Figure 12 where the thermal fluctuations are removed from the radiometric measurements at both V and H polarization. Also here the

periodic peaks at H polarization are due to effect of sun emission reflected from the surface and entering in the antenna pattern.

Scatter plot of Figure 13 points out the correlation between the antenna brightness temperature and cable physical temperature before and after the application of the temperature correction procedure. It can be noticed that while both temperatures are extremely correlated (R^2= 0.91) before the correction they are almost uncorrelated after the correction (R^2= 0.06). It is indeed expected that the measured Tb doesn't depends on cables' temperature.

It should be remembered that, as explained in [7], the minimization for the cable losses is applied for the different period of the years since we notice that the losses are temperature dependent and change in time. It is also worth pointing out that, because of the high thermal excursion of the cables, the estimates of L does not provide real values of the cable loss but a general value to minimize the thermal fluctuation effect. This includes the modification of matching between cables an antenna outputs and the receiver because of the temperature change. However, this correction is effective for the purpose of this study.

The values of the power loss L1, L2 calculated by the minimization procedure, are reported in Table 1 for V- and H- pol for different periods of the year.

Table 1: Values of (L1, L2) obtained after the compensation of the thermal effect

Date	L1v	L1h	L2v	L2h	Cal type
1/1/2015 - 2/3/2015	0.9	0.92	1	1	NOISE
4/3/2015 - 30/3/2015	0.9	0.85	1	1	NOISE
4/4/2015 - 5/5/2015	0.88	0.8	1	0.89	NOISE
5/5/2015 - 31/5/2015	0.9	0.9	0.88	0.88	NOISE
1/6/2015 - 29/8/2015	0.89	0.83	0.95	0.86	NOISE
30/08/2015 - 23/09/2015	0.87	0.87	0.85	0.93	NOISE
25/09/2015 - 1/12/2015		0.9		0.92	NOISE
1/12/2015 – 31/12/2015	0.8	0.95	0.91	0.89	TH/TC

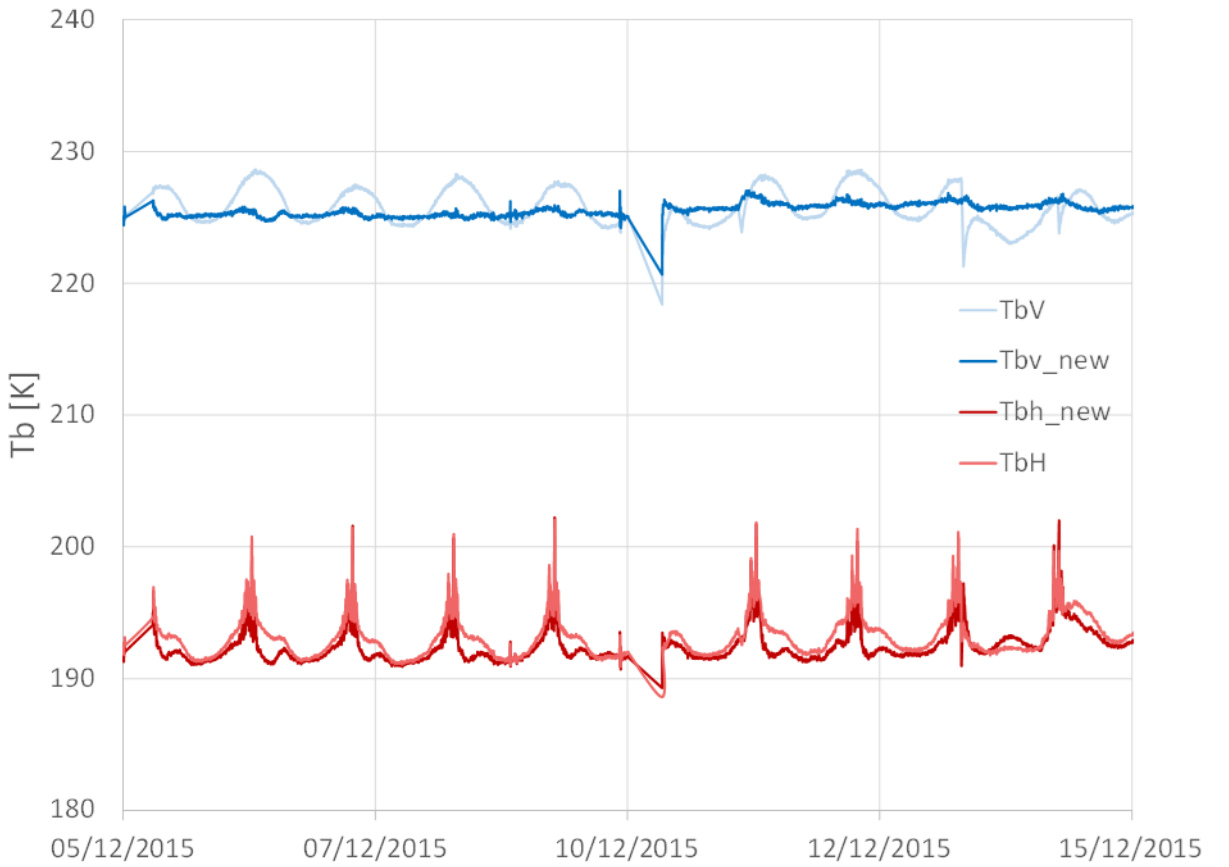

Figure 12: example of the Tb correction after temperature variations, showing original data and processed data at V-pol (blue and bright blue respectively) and H-pol (red and rose).

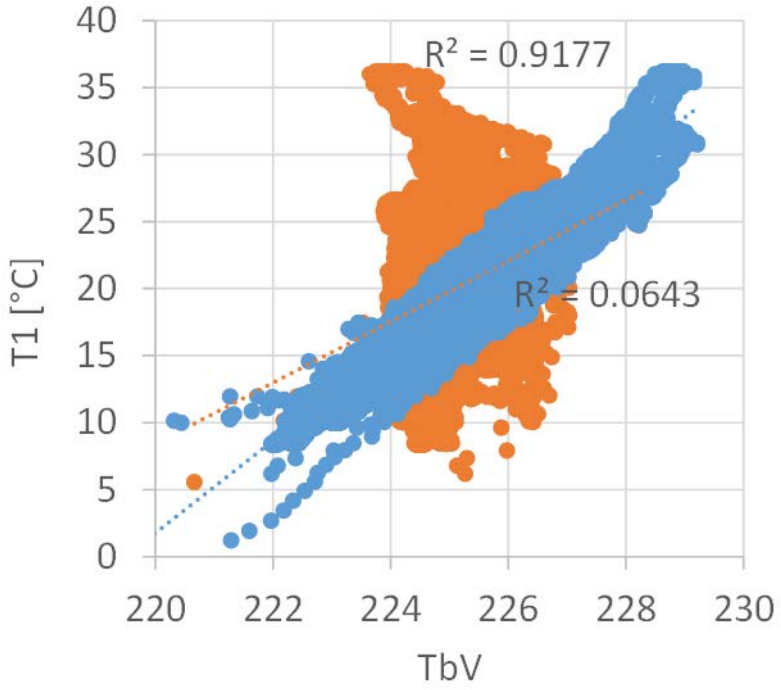

Figure 13: Tb correlation with the cable temperature before the correction (in blue) and after the correction (in orange).

4.3 DATA ANALYSIS

Brightness temperature of processed data is shown in Figure 14 at V and H polarization. The total time series from 1/1 to 15/12/2015 contains data averaged over 3 minutes (1 sample every 10 seconds) for a total of 124342 points. As pointed out previously, some of the V-pol acquisition have been corrupted by the switch failures, nevertheless about 60% of the data are preserved. Almost all the acquired data (93% of the total) are available at H-pol. Low values Tb (i.e. near to zero) observed in some period of the year represent the clear sky observation performed in 1/4 April, 14/19 May, 4/6 June, 12/21 Nov and 19/23 Dec. Even in this case some of the corrupted data are removed after the processing.

It must be considered that the high Tb variability observed for data collected in November on clear sky is motivated by the different incidence angles used in the measurements and the presence of the sun in the antenna lobe. As observed in the previous years, the fluctuation of H polarization in fall, summer and spring are due to the sun emissivity contribution reflected by the surface. In order to analyze data collected at 42° of incidence angle, we removed these data from the time series. It's worth noticing that the solar effect is maximum when the sun reaches in the same azimuthal plane of the antenna. The time series at 42° is shown in Figure 15. Picture shows that V polarization is stable and in line on what observed in the last seasons. A lower quality of data (more dispersion around their mean value) can be observed from April 17 to December 1st after the switch failures. The H pol. instead is more irregular and presents some fluctuations along the season. Recent results (Leduc-Leballeur, 2016) pointed out that those fluctuations are due to the modification of the snow surface properties which are also observed by SMOS.

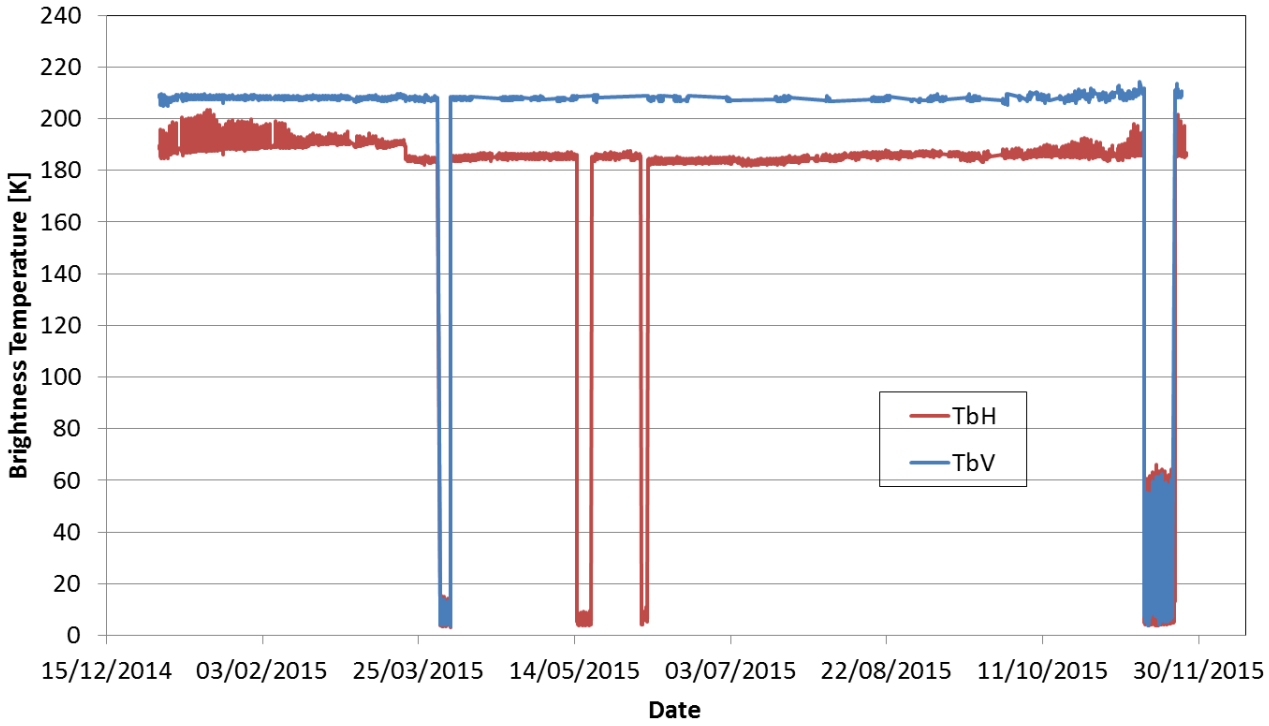

Figure 14: Brightness temperature recorded on 2015 for V-pol (in blue) and H-pol (in red)

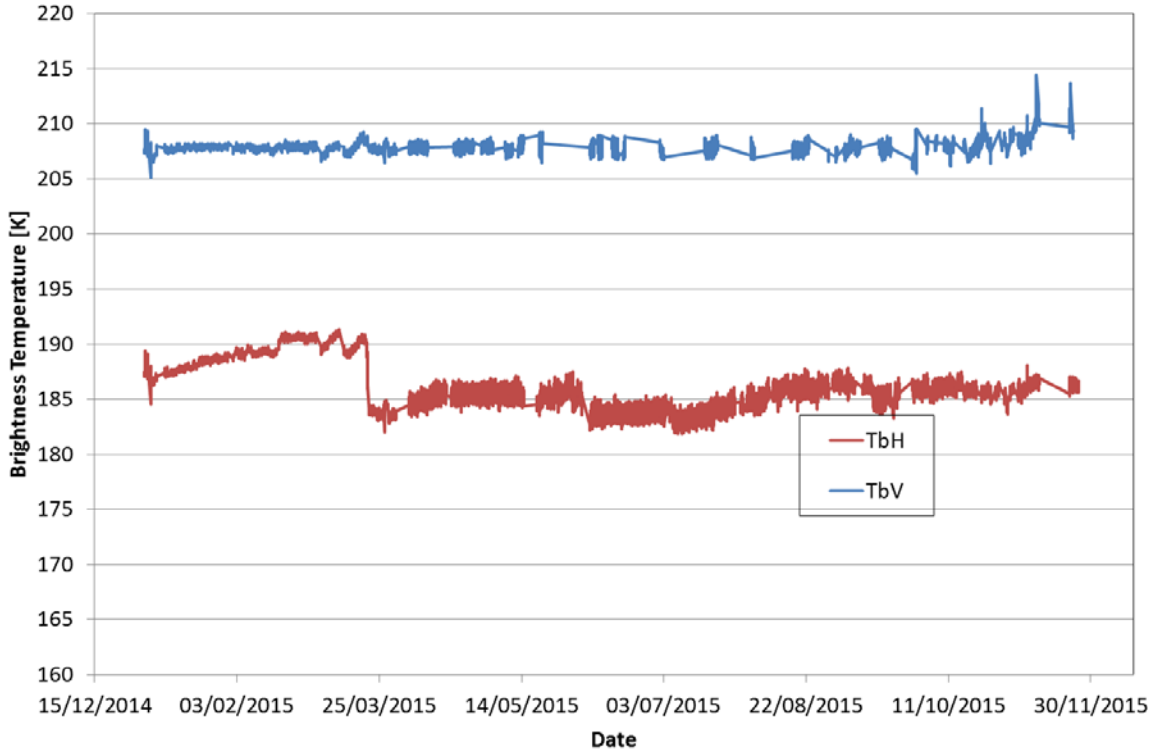

Figure 15: Brightness temperature recorded on 2015 for V-pol (in blue) and H-pol (in red) at 42° of incidence angle

A big drop (of about 5K) at H pol have been monitored at the end of March and also observed by SMOS. This event is followed by smaller ones at the beginning of June and July. Using meteorological data, hourly recorded in the AWS stations near the Concordia Base, we correlated the wind speed with the H-pol drops event (Figure 16). Figure contains the Tb at H polarization (top) and the wind speed (bottom). We represent in grey line, in both figures, when the wind speed overpass the 3-sigma average wind speed registered over the last three years for at least 5 hours. In some cases we notice a good correlation between the drop and the wind speed (i.e. 20 March and 7 July) while in in other cases (31 May and 13 September) the Tb drops are uncorrelated. The strong event of March 20 can be explained as follows: in the period January 1st to March 20 the wind speed was in generally moderate and caused a continuous accumulation of fresh snow on the surface , also because the formation of surface hoar, and then a decrease in snow density in the very first ice sheet layer. Theoretical computations confirm that this caused an increase in TbH. In March 20 strong wind determined the compaction of fresh snow, or the removing of the soft layer, an increase of snow density and then a sharp decrease of TBh. A more accurate analysis, using microwave models which can explain the physical modification of the H-pol and ground density measurements is in progress and will be included in a paper will be submitted to ISI journal in the next month (i.e October 2016).

The polarization index PI (PI = 2* (Tbv-Tbh)/(Tbv+Tbh)) is represented in Figure 17. In this case, the PI series is affected by the V- pol lack of data from 18/4 to 1/12. PI shows some variations which are mainly due to the modification of TbH series. The mean value of the PI along the year is 0.108 and is fully in line of what observed in 2014 (mean=0.110). On the other hand, due to the worst quality of V pol data, the standard deviation rises to 0.012, with respect to 0.0028 of the past year.

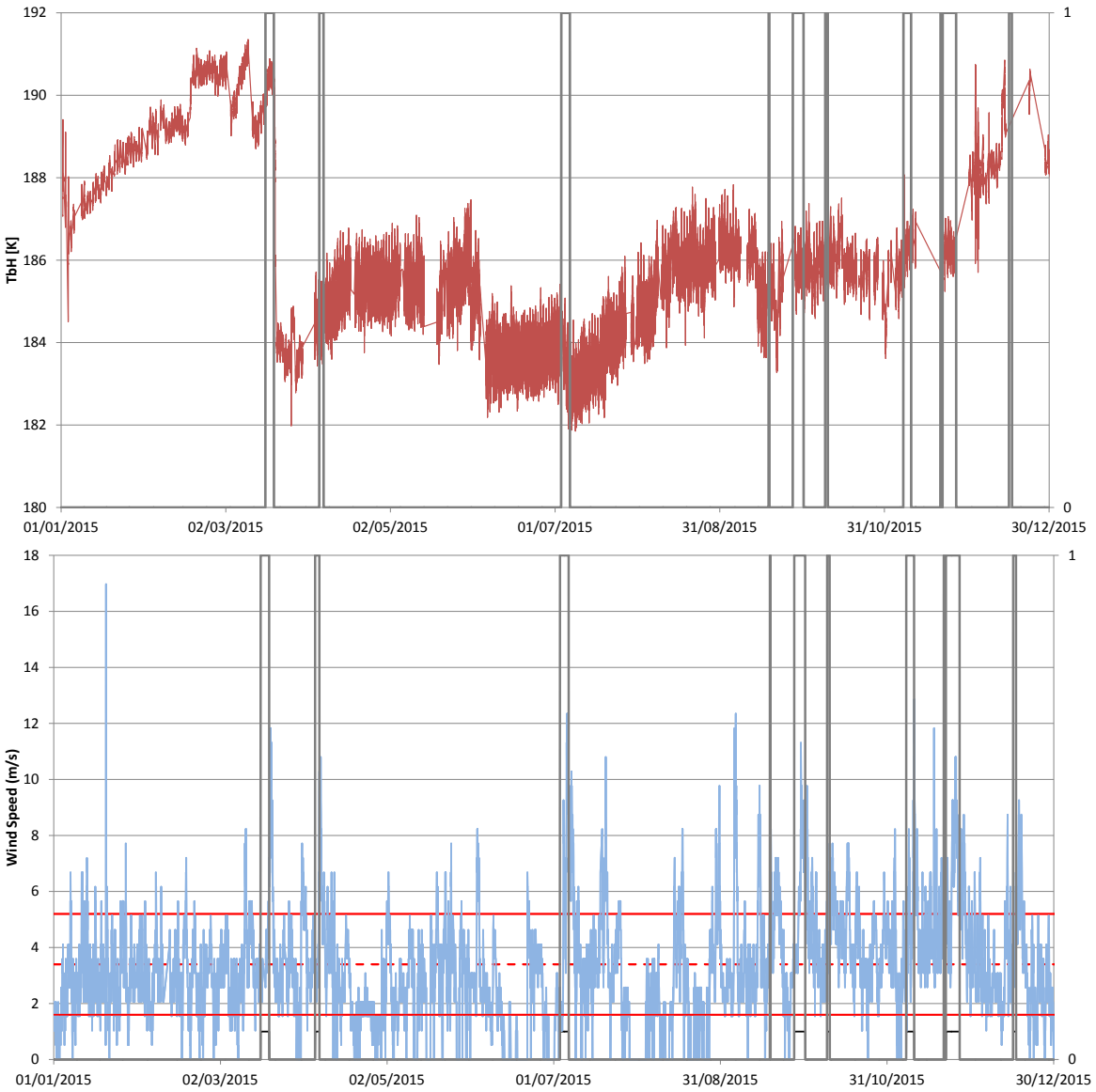

Figure 16: Top: temporal analysis of Th at 42° (in red) showing strong wind events which have last for a certain amount of time. The axis on the right has binary numbers, 1 when the wind event occurs or 0 elsewhere. Bottom: wind speed in m/s in bright blue, the annual average in red (dashed line) and the standard deviation in red (continuous line); on the right axes, the wind event occurrence.

Figure 17: Polarization Index as a function of time

Several tests are performed observing clear sky which is used as a reference for the absolute calibration. Because of the low quality of V- pol data also for sky observations, we decided to keep V- pol only in two cases in April 2015 and December 2015, while preserving H-pol for all the tests. The average and standard deviation values of the Tb are represented in Table 1 after removing the contribution of solar irradiation from the statistics. Similar values are measured from April to November at H- pol, whilst a slightly higher value is registered in December after the receiver substitution. This result can be explained by the lower angle of observation (115°instead of 120°) used for the calibrations tests. The 5° difference is motivated by a small inclination of the tower's structure which leads to a difference in the maximum observable angle.

It should be notice that the difference between the TB measured at 115° and 120° incidence angle depends on relative large antenna main lobe. This implies that the measurements collected at a nominal incidence angle are contaminated by the signal coming from other angles. Near to incidence angle of 90° this is particularly critical since there is a combination of very low signal coming from the sky (i.e. less than 10 K) to a signal higher than 150 K coming from the ice sheet. A small modification of incidence angle, such as the 5°, leads to a different contribution of the ice sheet signal then a different Tb value. It is expected that the measurements planned in the forthcoming summer campaign 2016 (i.e. cold sky calibration activities) will better characterize the antenna deconvolution process and then better quantifying the influence of the ice sheet in cold sky measurements.

An example of the calibrated sky observations in April is shown in Figure 18. The highest peaks in figure, about 13-15 K, are due to the pass of the sun in the antenna pattern, while the smallest peaks (about 10K) occurred because of the crossing of the galactic plane.

Table 1: Tb values obtained from sky observations in different periods of the year. Solar radiation is removed from statistics.

	TbV (K)	Std (K)	TbH (K)	Std (K)	Inc. Angle
April 2015	4.86	0.23	4.38	0.22	120
May 2015	NA	NA	4.98	0.21	120
Nov 2015	NA	NA	5.3	0.19	120
Dec 2015	6.5	0.1	6	0.1	115

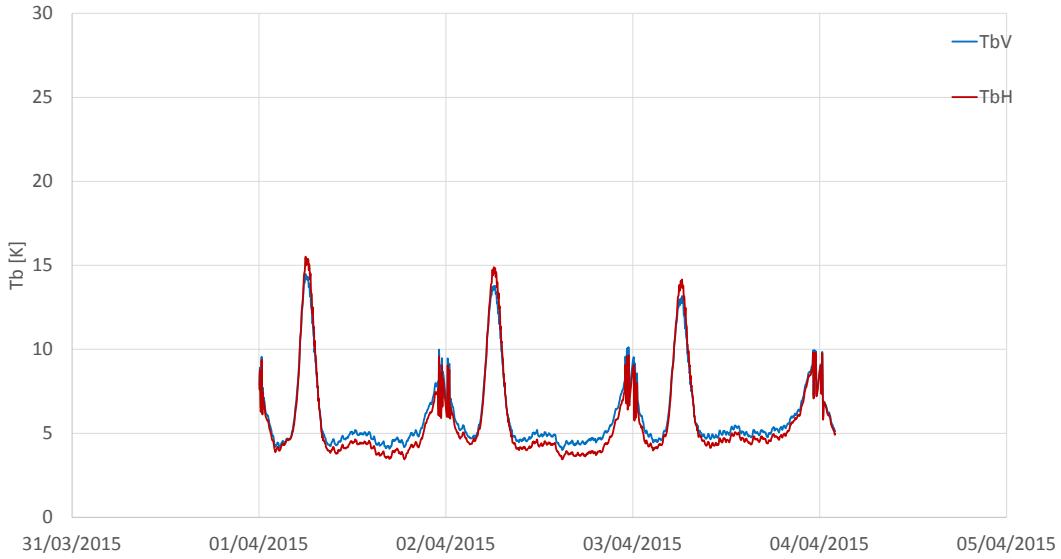

Figure 18: Calibrated value in clear sky conditions in April for V- pol (in blue) and H-pol (in red)

The data acquired at different incidence angle in 2015 are verified and compared with respect to previous years. Data collected from the beginning of the experiment in 2013 until present are represented in Figure 19. The 2015 angular trend show a good agreement with the past observations at V-pol. in the range 140-210K and confirm a good quality of inter-calibration. The H-pol value is around few K higher than the previous years and the difference is maximum at lower incidence angles while it tends to decrease at higher incidence. This is mainly due to the strong increase of H pol in March 2015.

The differences between the brightness temperature measured in each year and the average brightness temperature is represented in Figure 20 as a function of incidence angle. It can be observed that at V polarization the difference is on the order of ±1 K and doesn't change significantly as a function of

incidence angle except for 30° and 70°. The difference can be attributed both to natural Tb variability (annual fluctuation of the order of 1K are observed at V polarization) and absolute radiometer calibration. At H polarization the data measured in 2013 and 2014 are very similar while data measured in 2015 are quite different. Nevertheless this is not surprising because of the strong Tb values measured in March 2015 which influenced the data.

The quality of data is also checked by considering the standard deviation of brightness temperature, obtained every 3 minutes (Figure 21). The temporal series shows good performances of the receiver with an average standard deviation of about 0.22 K at both H and V polarization. Because of the switch performances degradation affecting the V polarization channel after April 18, the V pol presents several spikes after this date .

Internal temperature of the receiver is also monitored during the year. Figure 22 shows that the temperature of the receiver remains very stable in time exhibiting a dynamic range of around 0.2 °C over several months and lower than 0.4 °C for the first month of new receiver's acquisitions. The difference between the temperature measured in the two receivers can be explained as follows:

1-the RF sections doesn't have the same layout, then the temperature measured by the pt100 probes can be different

2-The PID set-up, which regulate the temperature inside the RF section, has been performed in two different conditions in the two receivers.

Detailed observations will be carried out during year 2016.

Antenna and RF cable temperatures as a function of time are shown in Figure 23. The temperature fluctuates of around 10 °C with respect to its mean value which is governed by the temporal variation of the temperature inside the radiometer. Winter values are more stable and controlled by the internal heaters in a temperature range around zero degrees.

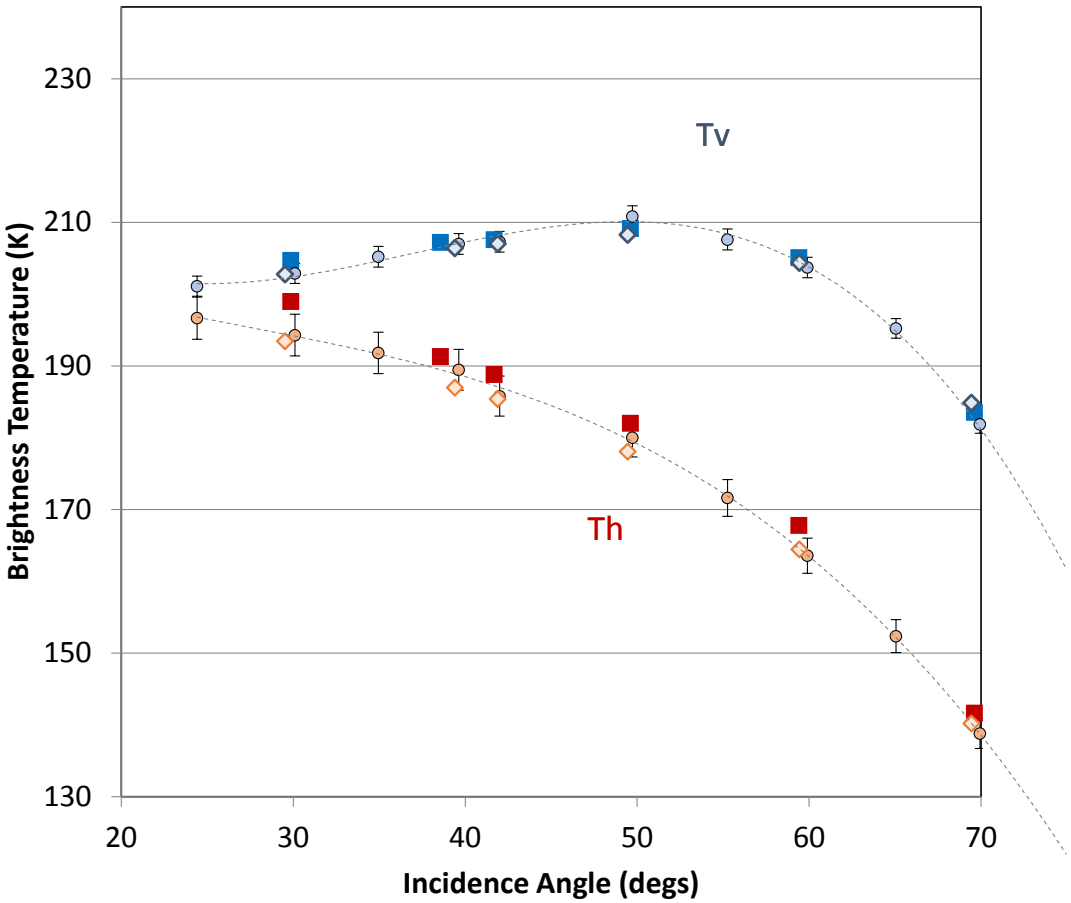

Figure 19: Brightness Temperature at V and H polarization as a function of incidence angle. Blue = V polarization: circle 2013 data, Diamond – 2014 data, square 2015 data. Red = H polarization : circle 2013 data, Diamond – 2014 data, square 2015 data.

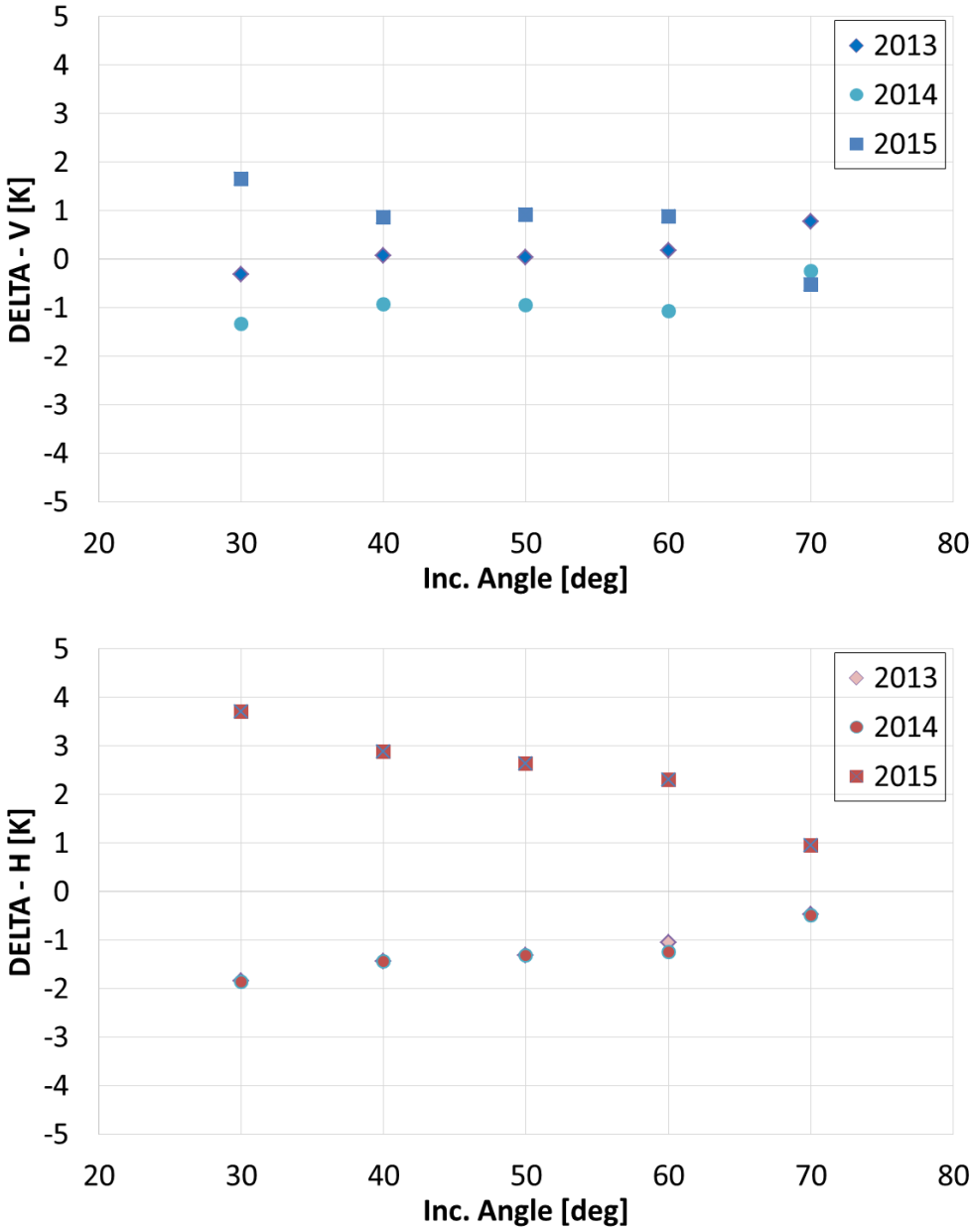

Figure 20: Difference of Brightness Temperature measured each year and 3 years average brightness temperature at V (top figure –blue symbols) and H (bottom figure – red symbols) polarization.

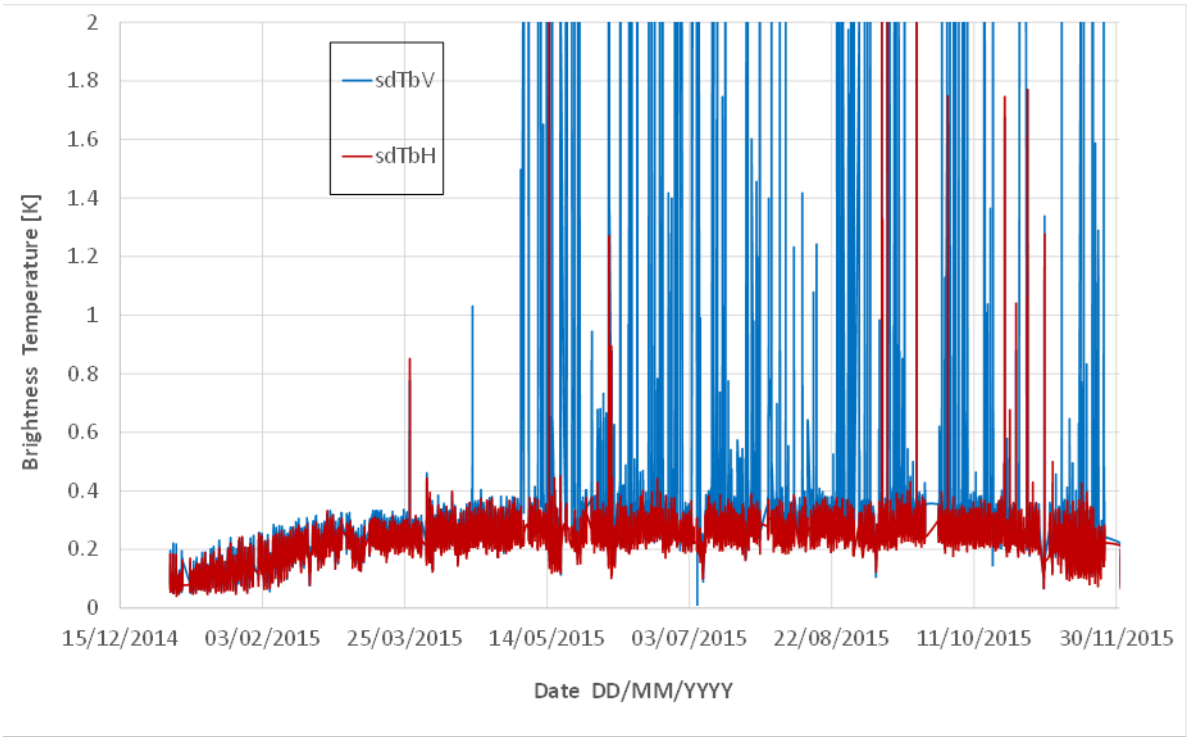

Figure 21: Brightness Temperature standard deviation at V (blue) and H polarization (red) as a function of time

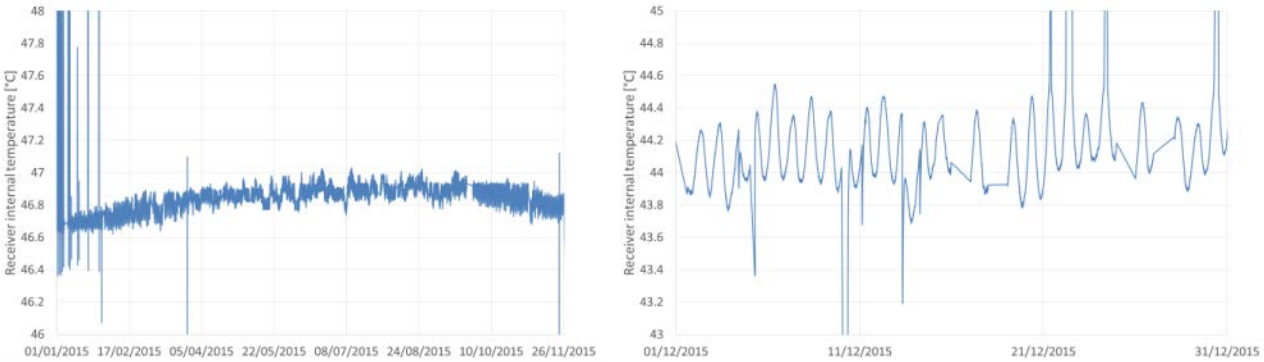

Figure 22: Temperature of the RF receiver in 2015, until 26/11 (on the left) and from 1/12 (on the right).

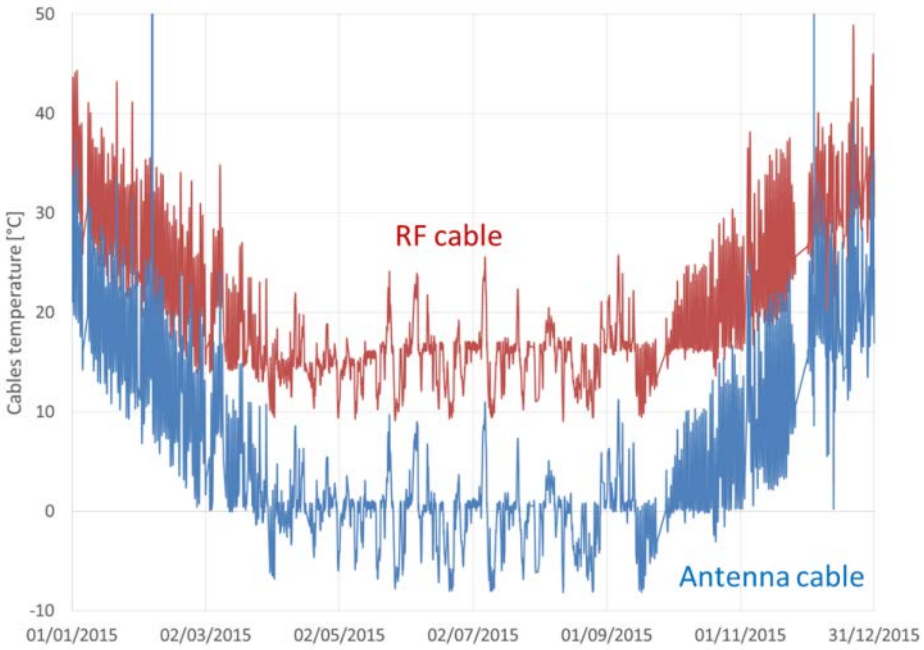

Figure 23: Temperature of the antenna's cable as a function of time.

4.4 PERFORMANCES OF THE NEW RECEIVER

In preparation of the 2015 summer campaign, activities were carried out at IFAC laboratories in order to properly set the new receiver and to characterize it. The new receiver is thermo-controlled at around 46°C and its inputs are connected to a 50 Ω matched loads. The loads are then placed in a thermo-controlled bath in order to modify theirs temperature.

In the first test the loads are placed at ambient temperature for a period of 10 days in order to quantify its temporal stability. Figure 24 represents the standard deviation of the brightness temperature at V pol and H pol. when the room temperature was about 20°C; the results pointed out a very good stability over time. The standard deviation was, on average, 0.14K at both V and H polarization. The temperature of the bath was then modified from -15°C to +45°C with 5°C step. The brightness temperature as a function of physical temperature of the bath is depicted in Figure 25. Data demonstrate the linearity of the receiver in the observed Tb range. Similar values are obtained at both polarization channels as expected.

The substitution of the receiver in Concordia was performed in 26/11. The first acquisitions show promising results and confirm what observed in laboratory tests. The comparison between the raw brightness temperatures acquired with the two receivers is presented in Figure 26, in two consecutive periods before and after the substitution. It can be observed that the spikes occurred at V polarization disappeared and the Tb values are in agreement with those measured in the previous period.

A comparison of the standard deviation of data acquired in three different years of the experiment with similar environmental characteristics (i.e. no sun irradiation and less thermal fluctuations) is shown in Figure 27. Data were acquired with the standard TH/TC calibration mode in January 2014 and January 2016 and with the noise source in January 2015. Mean standard deviation values calculated over each 20 samples for the same time period at H and V polarization for the three configurations are represented in

Figure 28. The average is very similar for the three cases, from 0.11K to 0.14K and for both polarizations. The stability will be further assessed in the prosecution of the 2016 campaign.

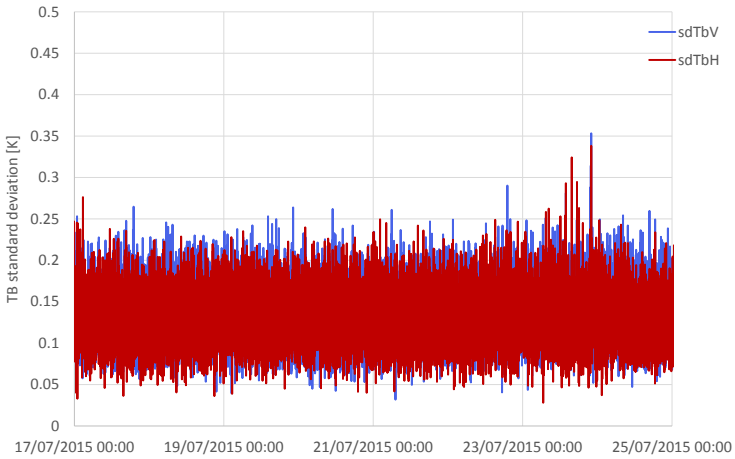

Figure 24: New receiver's standard deviation of the brightness temperature as a function of time for V pol (blue) and H pol (red). The receiver is attached to a 50 Ω matched load.

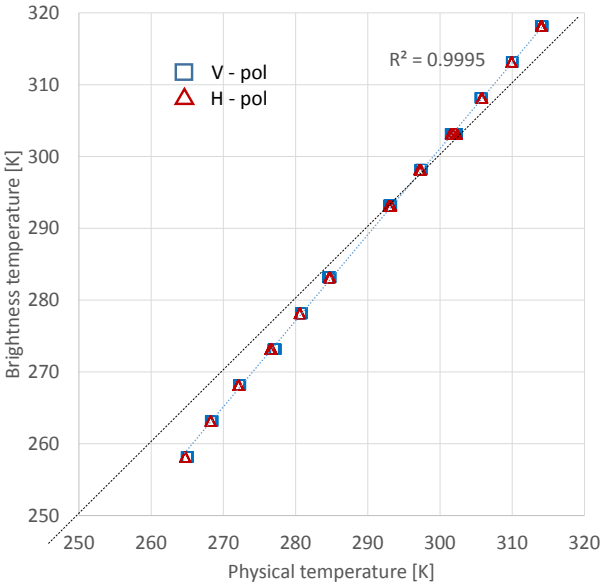

Figure 25: Brightness temperature measurements as a function of the physical temperature of a matched load placed in a thermal bath.

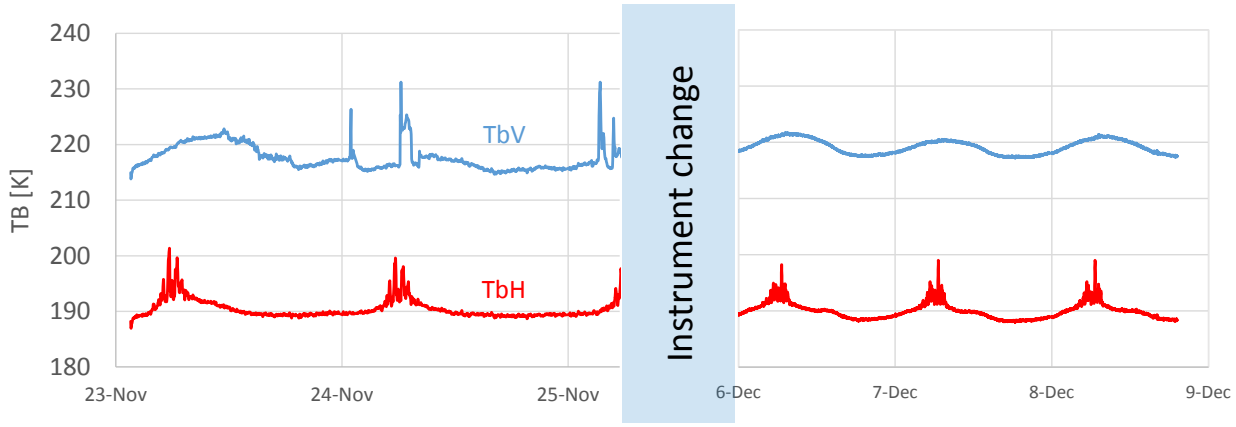

Figure 26: Brightness temperature before and after the receiver substitution, showing in blue V pol and in red the H pol.

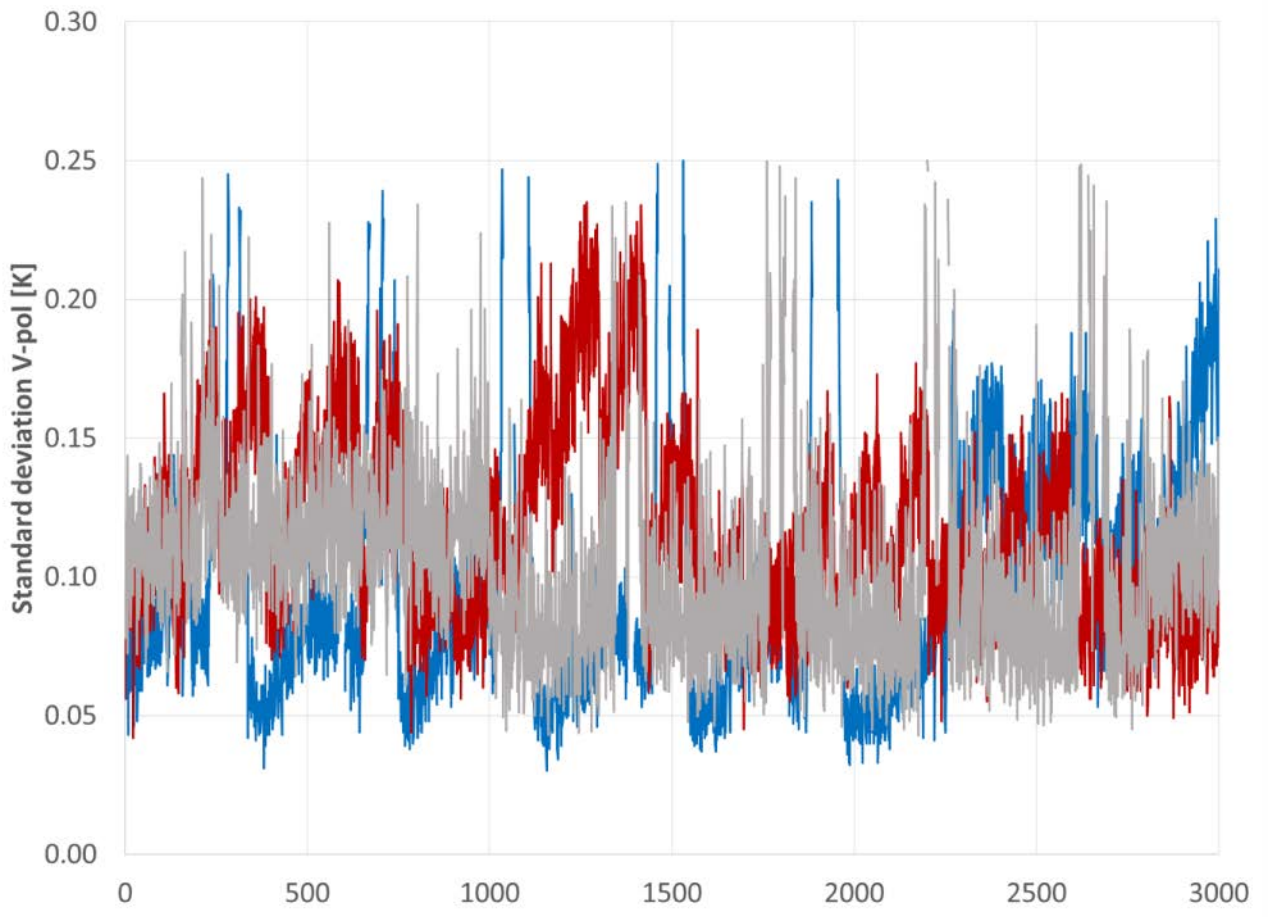

Figure 27: Radiometer performances at V-pol over one month of acquisitions in three different seasons, with the original receiver with the normal TH/TC calibration system (in blue) and with the noise source as a reference (in red) and the new receiver (in grey).

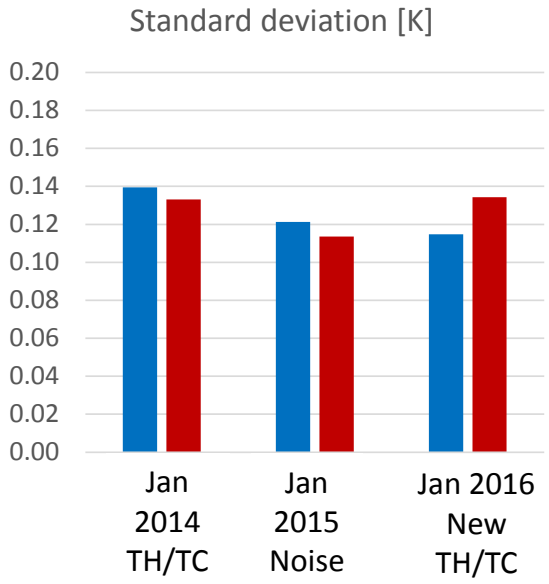

Figure 28: Average standard deviation for the three periods, showing V-pol in blue and H-pol in red.

4.5 Comparison with SMOS data

Deconvoluted RADOMEX data acquired during 2015 were compared to SMOS data and represented in Figure 29. SMOS data are in this case obtained with L1.C v620 data averaged over 9 pixels. Figure shows that data are in good agreement as temporal trends although the Tb at V polarization of SMOS is higher than DOMEX of about 3 K and lower than 1. 5 K at H polarization. Investigation to explain these differences is in progress. Standard deviation of SMOS is higher than DOMEX and in general, as observed in the past, is higher at H than V polarization. The Tb values measured by both sensors are represented in the following table.

	TBV (K)	St TBV (K)	TBH (K)	St TBH (K)
SMOS	212.52	1.48	186.75	2.63
DOMEX	209.61	0.52	188.023	1.90

It is interesting to observe that the slow Tb increase and the quick decrease from January to March 2015 at H polarization is measured by the two sensors. This implicitly means that the physical phenomena that caused this event is extended over a wide area (i.e. SMOS resolution is about 40 Km) and that DOMEX observation are representative of what observed by SMOS.

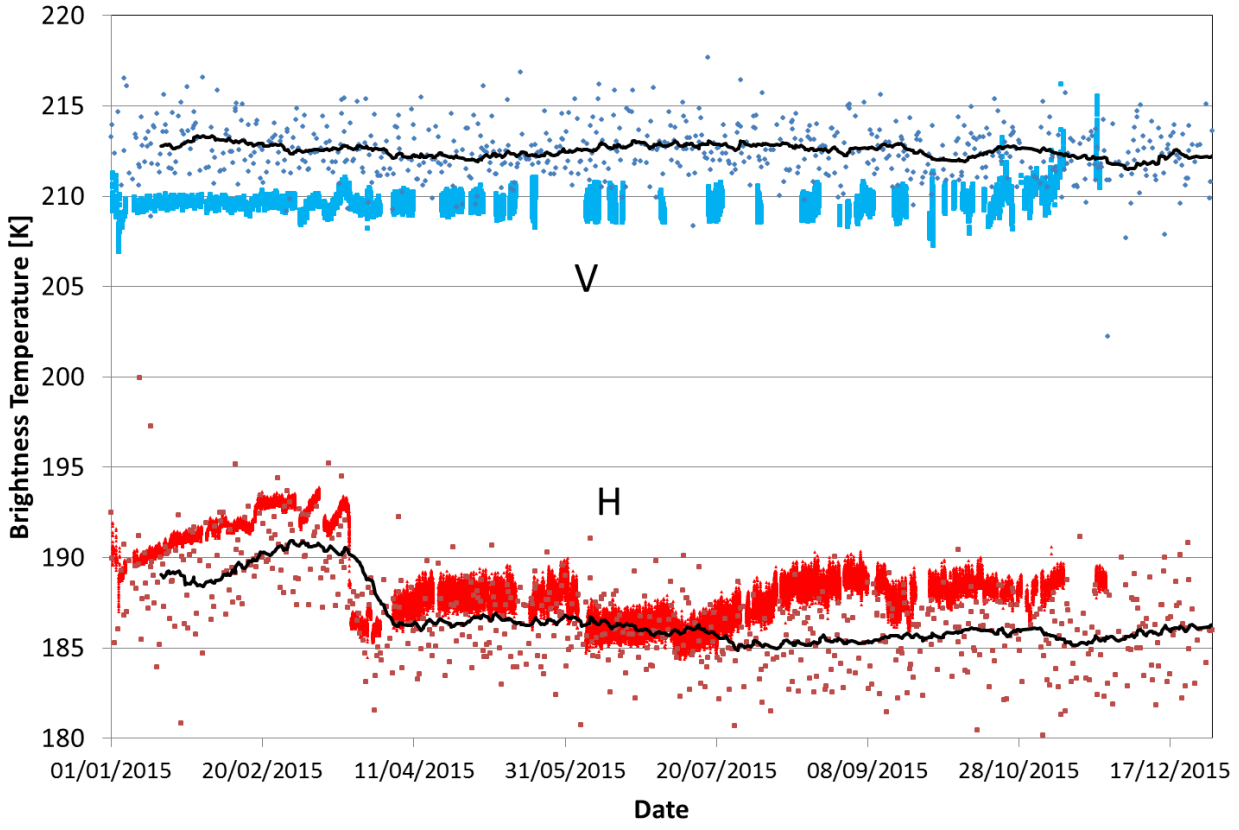

Figure 29: Brightness temperature measured by DOMEX (bright blue and red) and SMOS (blue and red dots) at H (red) and V (blue) polarization. The average value of SMOS is also represented in figure.

4.6 SNOW Data

Snow temperature measurements at Dome C are carried out continuously since the Domex-1 campaign in 2004. At present the snow temperature is collected by means of a Datalogger and a string of PT100 probes in the same site since Domex-2 (2009-10 summer campaign). The data collected during Domex-3 project are summarized hereinafter.

4.6.1 Snow temperature

The snow temperature measurement is collected continuously at different depths by means of permanent PT100 probes located in close to the US tower. The nominal depth of the probes is the following: 5, 10, 25, 75, 100, 150, 200, 250, 300, 400, 500, 600, 800 and 1000 cm. These are the depth of the probes at the time of deployment. Actually, due to the snow accumulation, the probes get deeper as time passed and snow accumulates. Only the probes placed in the first meter are realigned on every summer campaign. The snow accumulated on the surface since last 2013-14 summer campaign resulted to be 22.5cm, i.e. about 11 cm per year equivalent to approx. 3 cm of SWE.

Regarding the quality of the measurements, the datalogger works fairly well since the beginning of the experiment. Some small issues have been found during the last winter in the 800 cm deep probes when the data get noisy. In Dec 2014 the datalogger (but not the PT100 probes), was moved from the Helene shelter

to a new insulated box for logistic reasons thus a first explanation of the T800 noisy data could be that, during the winter the datalogger temperature was too much low and some sections of the instrument didn't work properly. To avoid this issue, during the last campaign the datalogger insulation was increased to 10 cm (where possible to 15 cm) with Styrofoam panels. Also T5, T25 and T600 channels experienced a quite significant loss of data. All of these problems were addressed in the last summer campaign and now the instrument is nominal.

Figure 30 represents the snow temperatures acquired at different depths for the entire Domex-3 experiment. It can be observed that data are continuous in time and, as expected, the temperature collected in the shallow part of the snow is highly influenced by the annual cycle of air temperature and sun radiation. As the temperature are collected deeper, this influence get weaker and the temperature get stable and converge to the mean annual value. This condition is well represented in Figure 31 where the average Temperature and the corresponding standard deviation are represented as a function of depth.
The IR temperature acquired in the same period is represented in Figure 32. It should be observed that, whereas the general year trend is similar throughout the years winter 2015 was colder than 2013 and 2014.

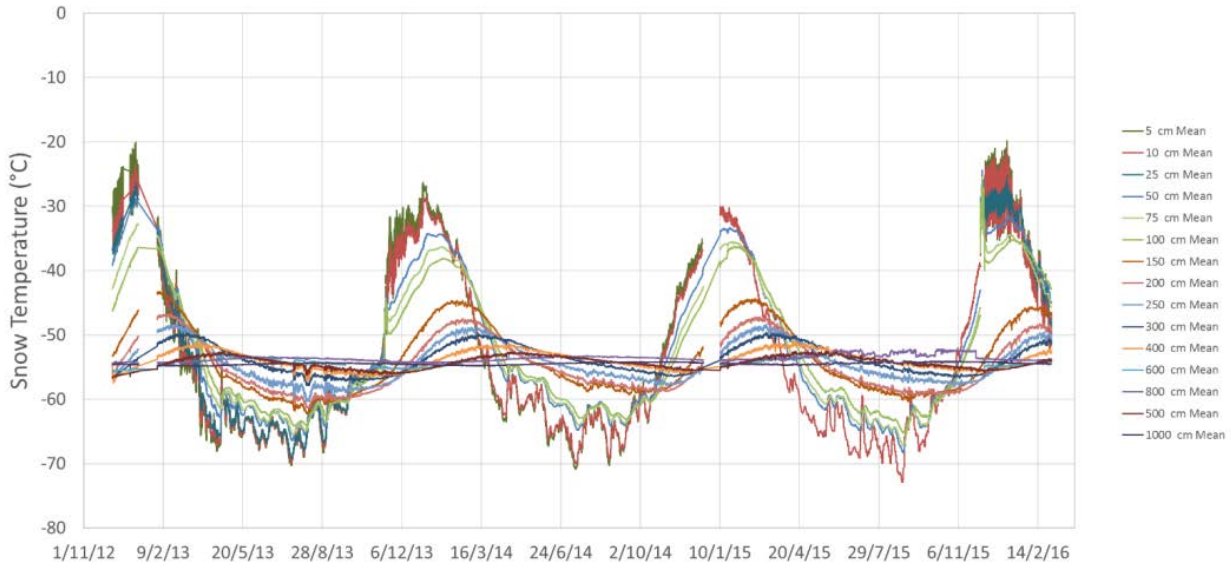

Figure 30: - snow temperature at different depths measured in 2014 year

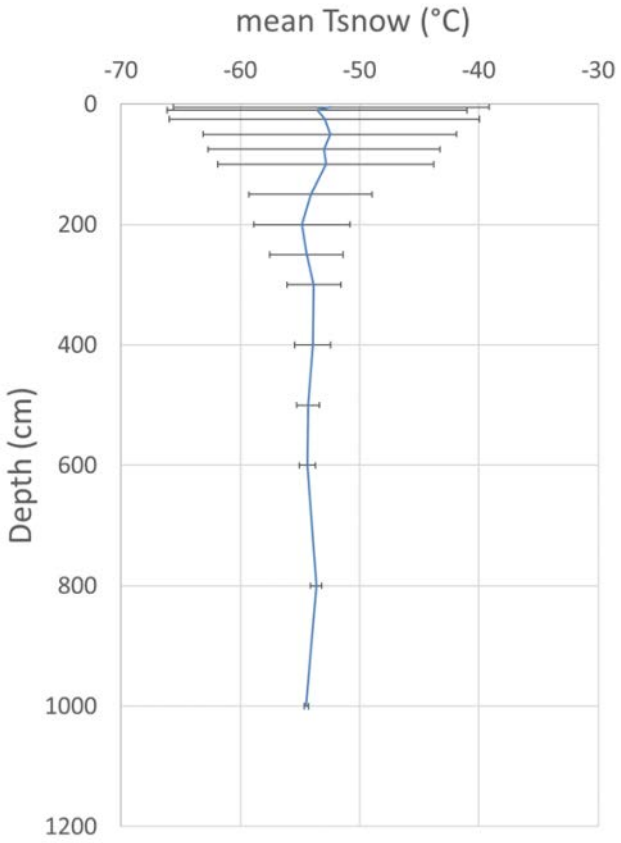

Figure 31: Average and standard deviation of the snow temperature as a function of depth for year 2014.

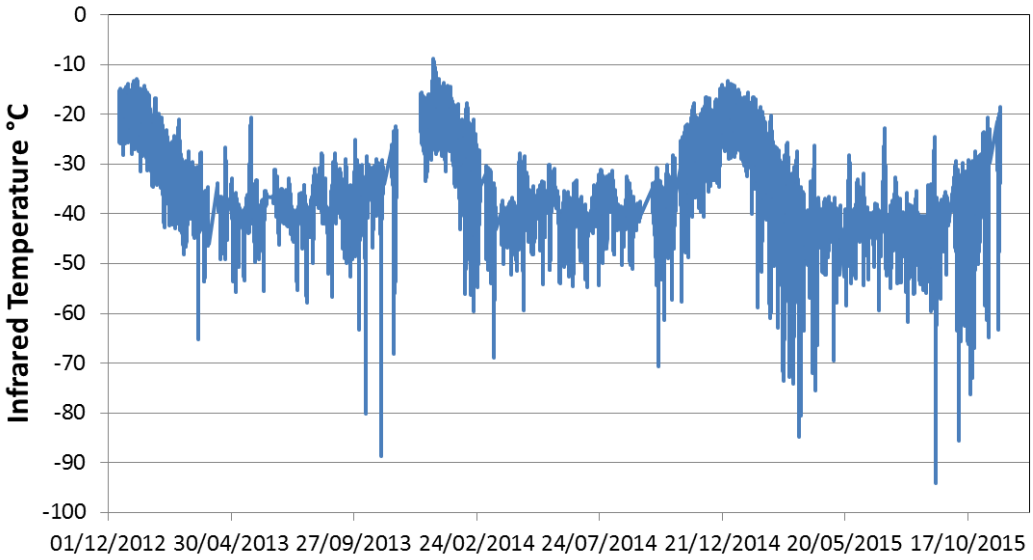

Figure 32: Infrared temperature.

5 DOMEX Publications

A list of paper published in 2015 related to DOMEX activity is contained here

Macelloni, G., Brogioni, M., Montomoli, F., Legovini, P., Casal, T. Analysis of L-band brightness temperature time series at DOME C – Antarctica (2015) International Geoscience and Remote Sensing Symposium (IGARSS), 2015-November, art. no. 7326713, pp. 4045-4048. DOI: 10.1109/IGARSS.2015.7326713

Brogioni, M., Macelloni, G., Montomoli, F., Jezek, K.C. Simulating Multifrequency Ground-Based Radiometric Measurements at Dome C-Antarctica (2015) IEEE Journal of Selected Topics in Applied Earth Observations and Remote Sensing, 8 (9), art. no. 7112470, pp. 4405-4417. DOI: 10.1109/JSTARS.2015.2427512

Tan, S., Aksoy, M., Brogioni, M., Macelloni, G., Durand, M., Jezek, K.C., Wang, T.-L., Tsang, L., Johnson, J.T., Drinkwater, M.R., Brucker, L.Physical Models of Layered Polar Firn Brightness Temperatures from 0.5 to 2 GHz (2015) IEEE Journal of Selected Topics in Applied Earth Observations and Remote Sensing, 8 (7), art. no. 7061406, pp. 3681-3691.DOI: 10.1109/JSTARS.2015.2403286

Jezek, K.C., Johnson, J.T., Drinkwater, M.R., Macelloni, G., Tsang, L., Aksoy, M., Durand, M. Radiometric approach for estimating relative changes in intraglacier average temperature (2015) IEEE Transactions on Geoscience and Remote Sensing, 53 (1), art. no. 2319265, pp. 134-143. DOI: 10.1109/TGRS.2014.2319265

6 References

[1] ESA-contract Technical Support for the Deployment of an L-band Radiometer at Concordia Station, Final Report, 2005

[2] ESA Contract:20066/06/NL/EL 22046/08/NL/EL, - Technical Support for the Deployment of an L-band radiometer at Concordia Station during DOMEX-2- - Final Report . 2011

[3] Esa Contract: 4000105872/12/NL/NF - Technical Support for the Deployment of an L-band radiometer at Concordia Station during DOMEX-2 – Proposal –July 2012

[4] Esa Contract: 4000105872/12/NL/NF - Technical Support for the Deployment of an L-band radiometer at Concordia Station during DOMEX-2 – Campaign Implementation Plan, Deliverable D2 – October 2012

[5] Esa Contract: 4000105872/12/NL/NF - Technical Support for the Deployment of an L-band radiometer at Concordia Station during DOMEX-2 – Readiness Review Report, Deliverable D3 – October 2012

[6] ESA-ESTEC Contract 4000105872/12/NL/NF Technical Support for the Long-Term Deployment of an L-Band Radiometer at Concordia Station, First Year Report , D6, February 2014

[7] ESA-ESTEC Contract 4000105872/12/NL/NF Technical Support for the Long-Term Deployment of an L-Band Radiometer at Concordia Station, Second Year Report , D6, June 2016

[8] ESA Contract 18060/04/NL/CB - Technical Support for the Deployment of an L-band radiometer at Concordia Station Final Report . May 2006

[9] MODELING L-BAND BRIGHTNESS TEMPERATURE IN CONNECTION WITH SNOW SURFACE PROPERTIES VARIATIONS AT DOME C, ANTARCTICA. Marion Leduc-Leballeur, Ghislain Picard, Giovanni Macelloni, Marco Brogioni, Laurent Arnaud, Arnaud Mialon, Yann H. Kerr –Microrad 2016

[10] Fierz, C., Armstrong, R.L., Durand, Y., Etchevers, P., Greene, E., McClung, D.M., Nishimura, K., Satyawali, P.K., and Sokratov, S.A., 2009. The International Classification for Seasonal Snow on the Ground. IHP-VII Technical Documents in Hydrology N. 83, IACS Contribution N1, UNESCO-IHP, Paris.

[11] De Franceschi, G. Alfonsi L., Romano V, "ISACCO: an Italian project to monitor the high latitudes ionosphere by means of GPS receivers", GPS Solution, DOI 10.1007/s10291-006-0036-6, 2006

[12] S. Kristensen, S. Søbjærg, E. Balling, N. Skou DOME Cair CampaignEMIRAD Data. Presentation & Analysis Version 1.0 – August 2013 –ESA project report.

This page is intentionally left blank

TECHNICAL SUPPORT FOR THE LONG-TERM DEPLOYMENT OF AN L-BAND RADIOMETER AT CONCORDIA STATION

DATA DESCRIPTION: MW –IR TEMPERATURE

JUNE 2016

EUROPEAN SPACE AGENCY STUDY CONTRACT REPORTS

ESTEC CONTRACT 4000105872/12/NL/NF

PREPARED BY

Giovanni Macelloni, Francesco Montomoli and Marco Brogioni

IFAC – CNR – SESTO FIORENTINO – ITALY

DATE: June 2016

This page is intentionally left blank

ESA STUDY CONTRACT REPORT			
EUROPEAN SPACE AGENCY STUDY CONTRACT REPORTS ESTEC CONTRACT 4000105872/12/NL/NF	TECHNICAL SUPPORT FOR THE LONG-TERM DEPLOYMENT OF AN L-BAND RADIOMETER AT CONCORDIA STATION		CONTRACTOR: IFAC-CNR
ESA CR ( )NO:	STAR CODE:	No of volumes: 1 This is volume no: 1	CONTRACTOR'S REF: MW-IR Temperature DataBase
ABSTRACT: This report contains the information of the MW-IR temperature data collected during DOMEX-3 experiment.			
The work described in this report was done under ESA Contract. Responsibility for the contents resides in the author or organisation that prepared it.			
AUTHORS: G. Macelloni, M. Brogioni, F.Montomoli (IFAC-CNR) ,			
ESA **STUDY MANAGER**: T.Casal		ESA BUDGET HEADING	

This page is intentionally left blank

1 TITLE

1.1 Data set identification

DOMEX-3 Microwave and Infrared Radiometers data.

1.2 Revision date of this document (dd/mm/yyyy)

07/06/2016

1.3 INVESTIGATOR(S)

Dr. Giovanni Macelloni
Earth Observation Department
Istituto di Fisica Applicata (IFAC)
Consiglio Nazionale delle Ricerche
Via Madonna del piano 10 - 50019 -Sesto Fiorentino (Fi) - Italy
Tel. + 39 055 5226495 – Fax + 39 055 5226467
E-mail: G.Macelloni@ifac.cnr.it

2 EQUIPMENT

2.1 Instrument description.

The measurements were carried out with IFAC microwave radiometer called RADOMEX, please refers to the Year report 2015 of the project for more information.

2.2 Platform (Satellite, Aircraft, Ground).

Ground

2.3 Key variables.

Microwave brightness temperature at 1.4 GHz (L-band), horizontal and vertical polarization, Infrared temperature (8-14 μm).

2.4 Instrument measurement geometry.

Data were collected from the tower-mounted radiometer from January 2015 to December 2015 at different incidence angles within the 20° - 130° range with respect to nadir (i.e 0° = nadir view) in the North-West direction. Different procedure have been followed for the acquisition as described in the Final Report and in the Experiment Support Plan of the project.

2.5 Manufacturer of instrument.

Instruments were designed and developed at IFAC CNR Firenze Italy

2.6 Calibration.

Calibration procedure was described in DOMEX-2 –Final report.

3 PROCEDURE

3.1 Data acquisition methods.

Data were collected automatically from the tower-mounted radiometer 24 hours/day. Data acquisition and platform movement were automatically controlled by means of a PC placed in the box; and the experiment was monitored remotely using a Local Area Network connection.

The following parameters were used for the acquisitions:
Integration time (measurement and calibration): 4 second
Number of measurements between calibration: 8 (4 H and 4 V)
Measurement Time (for each position): variable

IMPORTANT NOTE : In the dataset is represented the number of measurements, Tb mean value and standard deviation collected at each single position.

3.2 Spatial characteristics.

3.2.1 Spatial coverage.

Data were acquired at a fixed position at,:

Coordinates: 75.0989°S 123.3005°E

Altitude: 3250 M

The antenna foot-print (HPBW) ranged from 10x14 m^2 at θ = 20° to 10 x 160 m^2 at θ = 70° .

3.2.2 Spatial resolution.

Please refers to Experiment Implementation Plan

3.2.3 Temporal characteristics.

Please refers to Experiment Implementation Plan

3.2.4 Temporal coverage.

Data represented in this dataset were acquired from January 2015 to December 2015

4 DATA DESCRIPTION

4.1 Table definition with comments.

The data base is contained in the file DOMEX_3_THIRDYEAR_2015_MWDATA.txt in ASCII format.

It could be easily opened with MS Excel or Matlab.

The files are composed by a table of 124342 Rows + 1 (header) and 37 Columns

Column description:

c1 = Date – time DD/MM/YY hh:mm
c2 = Number of samples
c3 = Sun zenith position (degs)
c4 = Sun angular position (degs)

c5 = Quality flag; 0 = quality check passed; 1 = quality check not passed only for V-pol; 2 = quality check not passed only for H-pol; 3 = quality check not passed
c6 = sun flag; 0 = sun not in front of the antenna; 1 = sun in the antenna pattern
c7 = calibration scheme; 1 = frequent calibration hot and cold load; 2 = frequent calibration fixed gain, cold load; 3 = frequent calibration cold load and noise source.
c8 = TVL= Brightness Temperature L band – Vertical polarization (K)
c9 = Stdev TVL= Standard deviation of #c8 (K)
c10 = THL= Brightness Temperature L band – Horizontal polarization (K)
c11 = Stdev THL= Standard deviation of #c10 (K)
c12 = Theta = Incidence Angle (degrees)
c13 = SdevTheta = Standard deviation of #c12 (degs)
c14 = Theta = Azimuth Angle (degrees)
c15 = SdevTheta = Standard deviation of #c14 (degs)
c16 = Tir= Temperature of the calibrator of IR sensor (°C)
c17 = Stdev Tir= Standard deviation of #c16 (°C)
c18 = Temperature of Tns internal to the Radiometer receiver
c19 = Stdev Tns= Standard deviation of #c18 (°C)
c20 = Temperature of Tsw internal to the Radiometer receiver
c21 = Stdev Tsw= Standard deviation of #c20 (°C)
c22 = Temperature of Tcables1 internal to the Radiometer receiver
c23 = Stdev Tcables= Standard deviation of #c22 (°C)
c24 = Temperature of Tcables2 internal to the Radiometer receiver
c25 = Stdev Tcables= Standard deviation of #c24 (°C)
c26 = Temperature of T_H_omt connector
c27 = Stdev T_H_omt= Standard deviation of #c26 (°C)
c28 = Temperature of T_V_omt connector
c29 = Stdev T_V_omt= Standard deviation of #c28 (°C)
c30 = Temperature of T_H_rad connector
c31 = Stdev T_H_omt= Standard deviation of #c30 (°C)
c32 = Temperature of T_V_rad connector
c33 = Stdev T_V_rad= Standard deviation of #c32 (°C)
c34 = Temperature of T_OMT
c35 = Stdev T_ant= Standard deviation of #c34 (°C)
c36 = Temperature of Antenna front part
c37 = Stdev T_ant= Standard deviation of #c36 (°C)

- Missing data are identified as NaN

5 DATA QUALITY

5.1 Data Manipulations

As described in detail in the DOMEX Final Report the data at L band were processed and calibrated.

5.2 Sources of error.

The errors in the measurement were mainly related to the data post-processing. The adopted procedure is described in the Final Report of the project.

5.3 Quality assessment.

The minimum detectable temperature variation of the radiometer (sensitivity) was 0.3 K (with τ = 2 sec), and the accuracy (repeatability) was better than 0.5 K over a period of 30 days.

5.4 Quality flag definition.

The quality flag (column # c5 of the file) is defined as follows:
0 - Tb standard deviation computed over number of samples defined in column # c2 at V and H pol. Is lower than 1 K
1 - Tb standard deviation computed over number of samples defined in column # c2 at V pol. Is higher than 1 K
2 - Tb standard deviation computed over number of samples defined in column # c2 at H pol. Is higher than 1 K
3 - Tb standard deviation computed over number of samples defined in column # c2 at V and H pol. Is higher than 1 K.

A value higher than 0 imply a degradation of the measure.

6 REFERENCES

Technical Support for the Long-Term Deployment of an L-Band Radiometer at Concordia Station Yearly Report – Third Year Report, June 2016 EUROPEAN SPACE AGENCY STUDY
ESTEC Contract 4000105872/12/NL/NF –Macelloni et. Al

7 DATA POLICY

The participants (IFAC and CVA) have the exclusive right of access to and exploitation of data lather than 6 months after the end of the project (presentation of the final report). After this date dissemination of the dataset will be performed by ESA under the control and with the approval of IFAC.

TECHNICAL SUPPORT FOR THE LONG-TERM DEPLOYMENT OF AN L-BAND RADIOMETER AT CONCORDIA STATION

DATA DESCRIPTION: SNOWTEMPERATURE

MARCH 2016

EUROPEAN SPACE AGENCY STUDY CONTRACT REPORTS

ESTEC CONTRACT 4000105872/12/NL/NF

PREPARED BY

Giovanni Macelloni, Simone Pettinato, Francesco Montomoli and Marco Brogioni

IFAC – CNR – SESTO FIORENTINO – ITALY

DATE: March 2016

This page is intentionally left blank

ESA STUDY CONTRACT REPORT			
EUROPEAN SPACE AGENCY STUDY CONTRACT REPORTS ESTEC CONTRACT 4000105872/12/NL/NF	TECHNICAL SUPPORT FOR THE LONG-TERM DEPLOYMENT OF AN L-BAND RADIOMETER AT CONCORDIA STATION		CONTRACTOR: IFAC-CNR
ESA CR ( )NO:	STAR CODE:	No of volumes: 1 This is volume no: 1	CONTRACTOR'S REF: Snow Temperature DataBase
ABSTRACT: This report contains the information of the snow temperature data collected during DOMEX-3 experiment.			
The work described in this report was done under ESA Contract. Responsibility for the contents resides in the author or organisation that prepared it.			
AUTHORS: G. Macelloni, M. Brogioni, S.Pettinato (IFAC-CNR)			
ESA **STUDY MANAGER**: T.Casal		ESA BUDGET HEADING	

This page is intentionally left blank

1 TITLE

1.1 Data set identification

DOMEX-3 Snow Temperature Data

1.2 Revision date of this document (yyyy/mm/dd)

2016/03/02

2 INVESTIGATOR(S)

Dr. Giovanni Macelloni
Earth Observation Department
Istituto di Fisica Applicata (IFAC)
Consiglio Nazionale delle Ricerche
Via Madonna del piano 10 - 50019 -Sesto Fiorentino (Fi) - Italy
Tel. + 39 055 5226495 – Fax + 39 055 5226467
E-mail: G.Macelloni@ifac.cnr.it

3 EQUIPMENT

3.1 Instrument description.

The measurements were carried out with LSI LASTEM –data logger. –Model EL 305 and EL 105, Probes: PT100 Din-A
Please refers to http://www.lsi-lastem.it for more information.

3.2 Platform (Satellite, Aircraft, Ground).

Ground

3.3 Key variables.

Snow Temperature measured at different depth (range 0-10 m)

3.4 Instrument measurement geometry.

The temperature profile of the first 10 m of the snow pack was measured by using 10 probes. The probes (PT100 –DIN-A) were placed at different depths as described Table 1Table .

Table 1

Probe N	Depth (cm)
1	5
2	10
3	25
4	50
5	100
6	150
7	200
8	250
9	300
10	400
11	500
12	600
13	800
14	1000

3.5 Manufacturer of instrument.

Instruments were designed and developed by LSI-LASTEM (Italy).

4 PROCEDURE

4.1 Data acquisition methods.

Data were collected automatically by the data logger.

Data were acquired at each minute and recorded at each hour (mean, maximum, minimum).

IMPORTANT NOTE : In the dataset is represented the mean value are represented, the typical value of the standard deviation is less than 0.05 °C, maximum value is 0.1 °C

4.2 Spatial characteristics.

Spatial coverage.

Data were acquired at a fixed position at,:

Coordinates: 75.0989°S, 123.3005°E.

Altitude: 3250 m

Please refers to the Final Report of the project for more information

4.3 Temporal characteristics.

Temporal coverage.

Data represented in this dataset were acquired from January , 10 2015 to December , 31 2015.

5 5. DATA DESCRIPTION

Because of some problems affected the acquisition system, snow temperatures at 5 and 25 cm were not acquired in this time period. This problem was solved after December 4th, 2015. Snow temperature at 800 cm show an anomalous behavior.

5.1 Table definition with comments.

The data base is contained in the file **DOMEX3_snowtemp_database3.txt** as ASCII format.

It could be easily opened with MS Excel or Matlab.

The file is composed by a table 8533 rows + 1 (header) and 46 Columns.

Columns description:
c1 =Date – time YYYYMMDDTHHMMSS
c2 = T1= Minimum Temperature Probe 1 (50 cm) (°C)
c3 = T1= Mean Temperature Probe 1 (50 cm) (°C)
c4 = T1= Maximum Temperature Probe 1 (50 cm) (°C)
c5 = T2= Minimum Temperature Probe 1 (10 cm) (°C)
c6 = T2= Mean Temperature Probe 1 (10 cm) (°C)

c7 = T2= Maximum Temperature Probe 1 (10 cm) (°C)
c8 = T3= Minimum Temperature Probe 1 (100 cm) (°C)
c9 = T3= Mean Temperature Probe 1 (100 cm) (°C)
c10 = T3= Maximum Temperature Probe 1 (100 cm) (°C)
c11 = T4= Minimum Temperature Probe 1 (800 cm) (°C)
c12 = T4= Mean Temperature Probe 1 (800 cm) (°C)
c13 = T4= Maximum Temperature Probe 1 (800 cm) (°C)
c14 = T5= Minimum Temperature Probe 1 (600 cm) (°C)
c15 = T5= Mean Temperature Probe 1 (600 cm) (°C)
c16 = T5= Maximum Temperature Probe 1 (600 cm) (°C)
c17 = T6= Minimum Temperature Probe 1 (400 cm) (°C)
c18 = T6= Mean Temperature Probe 1 (400 cm) (°C)
c19 = T6= Maximum Temperature Probe 1 (400 cm) (°C)
c20 = T7= Minimum Temperature Probe 1 (300 cm) (°C)
c21 = T7= Mean Temperature Probe 1 (300 cm) (°C)
c22 = T7= Maximum Temperature Probe 1 (300 cm) (°C)
c23 = T8= Minimum Temperature Probe 1 (500 cm) (°C)
c24 = T8= Mean Temperature Probe 1 (500 cm) (°C)
c25 = T8= Maximum Temperature Probe 1 (500 cm) (°C)
c26 = T10= Minimum Temperature Probe 1 (5 cm) (°C)
c27 = T10= Mean Temperature Probe 1 (5 cm) (°C)
c28 = T10= Maximum Temperature Probe 1 (5 cm) (°C)
c29 = T11= Minimum Temperature Probe 1 (1000 cm) (°C)
c30 = T11= Mean Temperature Probe 1 (1000 cm) (°C)
c31 = T11= Maximum Temperature Probe 1 (1000 cm) (°C)
c32 = T12= Minimum Temperature Probe 1 (25 cm) (°C)
c33 = T12= Mean Temperature Probe 1 (25 cm) (°C)
c34 = T12= Maximum Temperature Probe 1 (25 cm) (°C)
c35 = T13= Minimum Temperature Probe 1 (150 cm) (°C)
c36 = T13= Mean Temperature Probe 1 (150 cm) (°C)
c37 = T13= Maximum Temperature Probe 1 (150 cm) (°C)
c38 = T14= Minimum Temperature Probe 1 (250 cm) (°C)
c39 = T14= Mean Temperature Probe 1 (250 cm) (°C)
c40 = T14= Maximum Temperature Probe 1 (250 cm) (°C)
c41 = T15= Minimum Temperature Probe 1 (200 cm) (°C)
c42 = T15= Mean Temperature Probe 1 (200 cm) (°C)
c43 = T15= Maximum Temperature Probe 1 (200 cm) (°C)
c44 = T16= Minimum Temperature Probe 1 (75 cm) (°C)
c45 = T16= Mean Temperature Probe 1 (75 cm) (°C)
c46 = T16= Maximum Temperature Probe 1 (75 cm) (°C)

- Missing data are identified as NaN

6 *DATA QUALITY*

6.1 Data Manipulations

Data were not manipulated

7 Sources of error.

Please refers to LSI-Lastem information

8 Quality assessment.

Please refers to LSI-Lastem information

9 REFERENCES

[1] LSI-LASTEM user manual (http://www.lsi-lastem.it/pdf/instum00031.pdf)

[2] TECHNICAL SUPPORT FOR THE LONG-TERM DEPLOYMENT OF AN L-BAND RADIOMETER AT CONCORDIA STATION

10 DATA POLICY

The participants (IFAC and CVA) have the exclusive right of access to and exploitation of data lather than 6 months after the end of the project (presentation of the final report). After this date dissemination of the dataset will be performed by ESA under the control and with the approval of IFAC.